

PREPARATION OF BROAD-GROUP CROSS SECTIONS FOR MULTIGROUP  
TRANSPORT CALCULATIONS - ANISN COMPUTER CODE OPTIONS

A Thesis

Submitted to the Graduate Faculty of the  
Louisiana State University and  
Agricultural and Mechanical College  
in partial fulfillment of the  
requirements for the degree of  
Master of Science

in

The Department of Nuclear Engineering

by

Farhad Dolatshahi  
B.S., Illinois Institute of Technology, 1975

May, 1978

DEDICATED TO

my family

#### ACKNOWLEDGMENT

The author wishes to express his sincere appreciation to Dr. Robert C. McIlhenny, Dr. Frank A. Iddings, and Dr. John C. Courtney for their constructive and useful suggestions in the preparation of this manuscript. Special thanks are due to my major professor Dr. Robert E. Miles for his invaluable guidance and assistance in the course of this study.

## TABLE OF CONTENTS

	Page
ACKNOWLEDGMENT. . . . .	iii
LIST OF TABLES. . . . .	vi
LIST OF FIGURES . . . . .	vii
ABSTRACT. . . . .	viii
 CHAPTER	
ONE. Introduction. . . . .	1
TWO. Master Cross-section Libraries. . . . .	5
2.1. DLC-2D 100 Group Neutron Cross-sections. . . . .	5
2.2. DLC-37 100 Neutron-21 Gamma Group Cross-sections for EPR Neutronics. . . . .	17
THREE. Data Retrieval from Master Cross-section Libraries. . . . .	28
FOUR. Collapsing the Fine-group Cross-sections into Broader Groups. . . . .	31
4.1. Preliminary Considerations . . . . .	31
4.2. APRFX-I Code . . . . .	33
4.3. ANISN Code . . . . .	40
4.4. DLC-2D Applications. . . . .	44
4.5. DLC-37/EPR Applications. . . . .	52
FIVE. Conclusions and Suggestions for Further Study . . . . .	61
REFERENCES. . . . .	64
 APPENDICES	
APPENDIX A. Fission Sources for Several Isotopes for the 99-group Energy Structure of DLC-2D Library . . . . .	66

TABLE OF CONTENTS (CONTINUED)

	Page
APPENDIX B. APRFX-I Partial Output. . . . .	76
APPENDIX C. Modifications to TAPE MAKER . . . . .	77
APPENDIX D. Creating a LOAD MODULE of ANISN . . . . .	78
VITA. . . . .	79

## LIST OF TABLES

Table	Page	
2.1	DLC-2D 99 Group Neutron Cross-section Multigroup Structure. . . . .	6
2.2	Data Organization of DLC-2D Cross-sections Illustrating Table Position, Cross Section Type, and Neutron Energy Groups. . . . .	10
2.3	DLC-2D Nuclei with Their Respective ID's - MAT ID Refers to the ID's on the Unformatted Library. . . . .	11
2.4	Thermal Group Cross-sections for Nuclei Contained in the DLC-2D 100 Group Neutron Cross-section Library . . . . .	13
2.5	Nuclei in DLC-2D 100-group Neutron Cross-section Library Requiring a Non-1/v Correction Factor at 293°K. . . . .	15
2.6A	DLC-37/EPR 100-group Neutron Multigroup Structure. . . . .	21
2.6B	DLC-37/EPR 21-group Gamma Multigroup Structure . . . . .	23
2.7	DLC-37/EPR Nuclei with Their ID's - MAT ID Refers to ID's on the Unformatted Tape . . . . .	24
2.8	Data Organization of EPR Cross-section, Illustrating Table Position, Cross-section Type, and Neutron Energy Groups. . . . .	27

## LIST OF FIGURES

Figure		Page
4.1	Example of APRFX-I Collapsing. . . . .	37
4.2	Input Cards for APRFX-I Collapsing Example . . . . .	38
4.3	Allocation of Tape Output for APRFX-I. . . . .	41
4.4	Broad Group Data Preparation for Multigroup Transport Codes. . . . .	45
4.5	Input to TAPE MAKER for P <sub>0</sub> Treatment of Cylindrical Reactor of Figure 4.1. . . . .	46
4.6	ANISN.SCANNER JCL Cards. . . . .	48
4.7A	Testing the Input Data for P <sub>0</sub> Case - No GIT Used . . .	50
4.7B	Test of the Input Data for P <sub>0</sub> Case - Using GIT . . . .	51
4.8	TAPE MAKER Card Input for the P <sub>3</sub> Case. . . . .	53
4.9	ANISN P <sub>3</sub> Data for the Problem in Figure 4.1. . . . .	55
4.10	TAPE MAKER Data for EPR Problem. . . . .	58
4.11	ANISN P <sub>3</sub> Data for EPR Problem. . . . .	59

## ABSTRACT

Sophisticated computer codes based on transport theory or probabilistic methods have been developed over the past twenty years for treating interactions of radiations with matter in complex systems. Master cross-section libraries for a given set of problems must be prepared by flux weighting point cross-section data. These libraries in turn must be collapsed into a few energy groups to permit reasonable computation times on even large computers. Collapsing the DLC-2D master cross-section library was demonstrated using APRFX-I\* code. The DLC-2D and DLC-37/EPR libraries were converted to unformatted binary tapes through LIBGEN and LIBGEN2\* for use with the discrete-ordinates code ANISN to generate two new master libraries named DLC2D.UNFORM\* and DLC37.UNFORM\*. ANISN was then used to collapse these cross-section data into broader groups. A special purpose program called TAPE MAKER\* is used to produce a "group independent" tape (GIT). Usage of this GIT to reduce the computer core requirements for ANISN-formatted multigroup transport or Monte Carlo codes is illustrated. Special programs T.M.TEST\* and ANISN.SCANNER\* were developed to check the accuracy of the input data prior to TAPE MAKER and ANISN runs to reduce the turn-around time.

The collapsed cross-sections are used in some ANISN example cases. The problems are outlined and the card images of the input

---

\* Codes modified or written for this thesis.



data and the Job Control Language (JCL) are listed. Numerous reference material are tabulated. These include material ID's, fine-group energy boundaries, fission spectra for fuel material, and similar data.

The significance of this thesis lies in its use as a formal introduction to cross-section data preparation for the multigroup transport codes. Frequently, these instructions are omitted from the computer code manuals. A major effort has been devoted to compile and gather in one place all the necessary information for the beginning user of these computer codes. The procedures involved are defined in relation to one another and in a continuous fashion.

## CHAPTER ONE

### Introduction

Studies of particle transport and shielding require extensive use of numerical methods and computer codes. The essence of the radiation transport through matter is usually based on a balance equation, as in Transport Theory, or a probabilistic counting process, as in Monte Carlo Methods, since these problems cannot be solved by analytical methods except under some very special circumstances. As a result, a major effort has been concentrated on the development of a number of accurate and general-purpose computer codes that can perform multigroup particle transport calculations.

One of the main difficulties in using these codes involves preparation of neutron (and sometimes gamma) interaction cross sections for a given problem. These master libraries, as they are called, are generated from the ENDF/B CROSS SECTION DATA<sup>(4, 5)</sup>, which consists of experimentally determined point cross-sections for different nuclei. The point cross-section data are processed according to the specific need of the user. The basic processes involved consist of obtaining from ENDF/B files the multigroup neutron and gamma cross-sections, gamma yields cross sections for photon-producing neutron interactions, neutron activity cross-sections and KERMA factors<sup>(12)</sup>. These data are arranged into a "coupled-cross section set" and then flux-weighted to form a many group master library of resonance-corrected application dependent cross sections.

The AMPX-II<sup>(3)</sup> modular code system available from the Radiation Shielding Information Center, Oak Ridge National Laboratory (ORNL), can be used for this purpose.

However, in many situations one does not have the luxury of generating an application dependent many group cross section set. In this case, depending on the expected neutron-energy spectrum in the system, one must choose from among different existing master libraries that which is most useful. For example, a set of cross-sections suitable for criticality study in a light water reactor will not be appropriate for first-wall considerations in a fusion system containing hot plasma, because the energy spectra are radically different.

Frequently, these cross-section data sets require an extremely large amount of computer core, which is usually not available to the user. Hence the next crucial step is to flux-weight these cross sections from a master library still further to create a smaller, or few-group, structure. This process is called collapsing the fine-group cross-sections into a broad-group set. The actual calculations involved in the process of collapsing the fine-group data are done by use of computer codes developed for this purpose. Once a set of collapsed cross-sections is available, they are inputted with the required format to the multigroup transport codes to perform calculations.

The sequence of steps described above constitute a guide line for this thesis, which begins with an introduction to the two master cross-section libraries currently available at the LSU Nuclear

Science Center. These are DLC-2D 100-group Neutron Cross Sections<sup>(6)</sup>, and DLC-37/EPR Coupled 100-group Neutron, 21-group Gamma Cross Sections<sup>(7)</sup>. Both libraries are constructed according to a  $P_8$ -Legendre polynomial approximation of scattering terms. This introduction will be followed by a description of the cross-section library-generation routines LIBGEN<sup>(8)</sup> and LIBGEN2, which are used to create a compiled unformatted binary data sets on magnetic tapes.

A brief description of the program APRFX-I<sup>(2)</sup> is presented thereafter. This code is used to collapse the DLC-2D fine-group cross-sections into a broader-group structure. APRFX-I was developed at the U. S. Army Nuclear Effects Laboratory. It employs a multi-group diffusion-theory calculation assuming a homogenous medium. The geometry of the system is taken under consideration via inputting a buckling-correction term, and the fluxes calculated by a straightforward diffusion equation solution which provides an estimate of the fine-group spectrum in cases where no previous information is available.

A major part of the remaining chapters is devoted to the utilization of the ANISN<sup>(1)</sup> program, a multigroup one-dimensional discrete-ordinates transport code. ANISN uses a transport-theory solution with anisotropic scattering in flux calculations; and, when invoking a built-in option, utilizes these fluxes to collapse the fine-group cross-sections through several iterations. The flux convergence criterion, the geometry and dimensions of the system, are all input. In addition, any fine-group library may be collapsed using ANISN. Thus the fluxes for a given problem are calculated with

a more accurate modeling than APRFX-I and utilizes the more exact transport theory methods. This also implies that the broad-group cross-sections are more accurate.

The use of these broad-group cross-section data is demonstrated by considering a few sample transport problems. Calculations are performed by ANISN code, and the cross-section input data are prepared by TAPE MAKER<sup>(8)</sup> routine. TAPE MAKER was developed at ORNL as an auxiliary routine to generate group independent set of cross-section data on tape. Using this code, the nuclide-organized cross-section libraries such as DLC-2D and DLC-37/EPR, are mixed to form macroscopic mixture cross-sections for each energy group. In an ANISN run then--rather than storing the whole cross-section matrix in the computer core--the data are stored for one group at a time. When the calculations for a group are performed, the data are replaced by the next group. This option greatly reduces the amount of the required storage, and makes it possible to work with a larger number of mixtures, higher  $P_{\ell}$  approximations, and more mesh spacings.

The example problems were chosen to avoid unnecessary complications and yet illustrate important considerations for realistic situations. In each case, after a brief description of the problem, the card image of the input data and the Job Control Language (JCL) commands are shown.

## CHAPTER TWO

### Master Cross-section Libraries

#### 2.1. DLC-2D 100 Group Neutron Cross-sections

The DLC-2D library was generated by R. Q. Wright of the ORNL Mathematical Division. It is based on ENDF/B Category I point cross-sections as released by the National Neutron Cross-section Center, Brookhaven National Laboratory. The ENDF/B data were processed by PSR-13/SUPERLOG<sup>(9)</sup> computer code to generate 100 group neutron cross sections. This process involved averaging the ENDF/B data over each specified group width. The assumption was made that the flux-weighting function had the shape of a fission spectrum joined at 0.067 MeV by a 1/E tail. The resonance contributions were calculated using the infinite dilution approximation when resonance data were available.

DLC-2D represents a  $P_8$  approximation to elastic scattering angular distributions. The 100-energy-group structure has a group 1 upper boundary of 14.92 MeV and a group 99 lower energy of 0.414 eV. The group boundary energies and lethargies are listed in Table 2.1. Group 100 serves as a thermal or sink group and only the down scatter in energy is represented. Lethargy is defined as  $\mu = \ln E_0/E$  where  $E_0$  is the energy of the most energetic neutron in the system and  $E$  denotes the energy variable. Since the average number of collisions per unit lethargy is a constant, the neutron slowing down and collision density is usually expressed as a function of lethargy rather than energy.

Table 2.1

DLC-2D 99 Group Neutron Cross-section  
Multigroup Structure

Group	Energy Range (eV)	Lethargy Range
1	1.3499E 07 to 1.4918E 07	-0.400 to -0.300
2	1.2214E 07	-0.300 -0.200
3	1.1052E 07	-0.200 -0.100
4	1.0000E 07	-0.100 0.000
5	9.0484E 06	0.000 0.100
6	8.1873E 06	0.100 0.200
7	7.4082E 06	0.200 0.300
8	6.7032E 06	0.300 0.400
9	6.0653E 06	0.400 0.500
10	5.4881E 06	0.500 0.600
11	4.9659E 06	0.600 0.700
12	4.4933E 06	0.700 0.800
13	4.0657E 06	0.800 0.900
14	3.6788E 06	0.900 1.000
15	3.3287E 06	1.000 1.100
16	3.0119E 06	1.100 1.200
17	2.7253E 06	1.200 1.300
18	2.4660E 06	1.300 1.400
19	2.2313E 06	1.400 1.500
20	2.0190E 06	1.500 1.600
21	1.8268E 06	1.600 1.700
22	1.6530E 06	1.700 1.800
23	1.4957E 06	1.800 1.900
24	1.3534E 06	1.900 2.000
25	1.2246E 06	2.000 2.100
26	1.1080E 06	2.100 2.200
27	1.0026E 06	2.200 2.300
28	9.0718E 05	2.300 2.400
29	8.2085E 05	2.400 2.500
30	7.4274E 05	2.500 2.600
31	6.7206E 05	2.600 2.700
32	6.0810E 05	2.700 2.800
33	5.5023E 05	2.800 2.900
34	4.9787E 05	2.900 3.000
35	4.5049E 05	3.000 3.100
36	4.0762E 05	3.100 3.200
37	3.6883E 05	3.200 3.300
38	3.3373E 05	3.300 3.400
39	3.0197E 05	3.400 3.500
40	2.7324E 05	3.500 3.600

Table 2.1 Continued

Group	Energy Range (eV)	Lethargy Range
41	2.4724E 05 to 2.7324E 05	3.600 to 3.700
42	2.2371E 05	3.700 3.800
43	2.0242E 05	3.800 3.900
44	1.8316E 05	3.900 4.000
45	1.6573E 05	4.000 4.100
46	1.4996E 05	4.100 4.200
47	1.3569E 05	4.200 4.300
48	1.2277E 05	4.300 4.400
49	1.1109E 05	4.400 4.500
50	8.6517E 04	4.500 4.750
51	6.7379E 04	4.750 5.000
52	5.2475E 04	5.000 5.250
53	4.0868E 04	5.250 5.500
54	3.1828E 04	5.500 5.750
55	2.4788E 04	5.750 6.000
56	1.9305E 04	6.000 6.250
57	1.5034E 04	6.250 6.500
58	1.1709E 04	6.500 6.750
59	9.1188E 03	6.750 7.000
60	7.1017E 03	7.000 7.250
61	5.5308E 03	7.250 7.500
62	4.3074E 03	7.500 7.750
63	3.3546E 03	7.750 8.000
64	2.6126E 03	8.000 8.250
65	2.0347E 03	8.250 8.500
66	1.5846E 03	8.500 8.750
67	1.2341E 03	8.750 9.000
68	9.6112E 02	9.000 9.250
69	7.4852E 02	9.250 9.500
70	5.8295E 02	9.500 9.750
71	4.5400E 02	9.750 10.000
72	3.5357E 02	10.000 10.250
73	2.7536E 02	10.250 10.500
74	2.1445E 02	10.500 10.750
75	1.6702E 02	10.750 11.000
76	1.3007E 02	11.000 11.250
77	1.0130E 02	11.250 11.500
78	7.8893E 01	11.500 11.750
79	6.1442E 01	11.750 12.000
80	4.7851E 01	12.000 12.250
81	3.7267E 01	12.250 12.500
82	2.9023E 01	12.500 12.750
83	2.2603E 01	12.750 13.000
84	1.7603E 01	13.000 13.250



Table 2.1 Continued

Group	Energy Range (eV)	Lethargy Range
85	1.3710E 01 to 1.7603E 01	13.250 to 13.500
86	1.0677E 01 1.3710E 01	13.500 13.750
87	8.3153E 00 1.0677E 01	13.750 14.000
88	6.4760E 00 8.3153E 00	14.000 14.250
89	5.0435E 00 6.4760E 00	14.250 14.500
90	3.9279E 00 5.0435E 00	14.500 14.750
91	3.0590E 00 3.9279E 00	14.750 15.000
92	2.3824E 00 3.0590E 00	15.000 15.250
93	1.8554E 00 2.3824E 00	15.250 15.500
94	1.4450E 00 1.8554E 00	15.500 15.750
95	1.1254E 00 1.4450E 00	15.750 16.000
96	8.7642E 01 1.1254E 00	16.000 16.250
97	6.8256E 01 8.7642E 01	16.250 16.500
98	5.3158E 01 6.8256E 01	16.500 16.750
99	4.1399E 01 5.358E 01	16.750 17.000

Weighting Function

$$1/E$$

Number of Groups - 99, plus 1 sink group. All data are downscatter.

Neutron transport calculations can be performed with DLC-2D data. These cross-sections are intended for use in ANISN-formatted (to be discussed in Chapter Three) multigroup transport or Monte Carlo codes which treat anisotropic scattering, and thus require a Legendre expansion to angular distribution of the scattering cross sections.

The DLC-2D data in card-image format on tape for each  $P_\ell$  value, consists of the one-dimensional fine-group constants  $\sigma_a$ ,  $\nu\sigma_f$ , and  $\sigma_t$ , and the two-dimensional elastic-scattering matrices. This data organization for each  $P_\ell$  cross-section set is illustrated in Table 2.2. The units are in barns ( $10^{-24}$  cm<sup>2</sup>). Positions 1 through 3 are assigned to  $\sigma_a$ ,  $\nu\sigma_f$ , and  $\sigma_t$  in the cross-section table; positions 4 through 103 are reserved for group-transfer constants. These tables are constructed in an ascending order of  $P_\ell$  values; i.e.,  $P_0, P_1, \dots, P_8$ . A 4-digit ENDF/B ID number is assigned to each nuclide. These nuclei are listed in Table 2.3.

The thermal-group cross sections  $\sigma_a$ ,  $\nu\sigma_f$ , and  $\sigma_t$  were not taken from ENDF/B library. These values are the Maxwellian-averaged absorption, scattering, and fission cross-sections at a temperature of 293°K (20°C), with  $\sigma_s$  assumed to remain constant over the thermal energy range. In cases where  $\sigma_a$  varies as  $1/v$ , the data were multiplied by the correction factor  $\sqrt{\pi/2}$ , and the results were used to calculate the thermal-group averages. In addition, some elements required a Non- $1/v$  correction. The values used for thermal group are listed in Table 2.4, and the nuclei requiring a Non- $1/v$  correction are shown in Table 2.5. When using these cross-sections

Table 2.2  
 Data Organization of DLC-2D Cross-sections Illustrating Table Position,  
 Cross Section Type, and Neutron Energy Groups

Position	Cross-section type	Groups:g			
		1	2	3	100
1	$\sigma_a$	$\sigma_a^1$	$\sigma_a^2$	$\sigma_a^3$	$\sigma_a^{100}$
2	$\nu\sigma_f$	$\nu\sigma_f^1$	$\nu\sigma_f^2$	$\nu\sigma_f^3$	$\nu\sigma_f^{100}$
3	$\sigma_t$	$\sigma_t^1$	$\sigma_t^2$	$\sigma_t^3$	$\sigma_t^{100}$
4	$\sigma_g \rightarrow g$	$\sigma_{1 \rightarrow 1}^1$	$\sigma_{2 \rightarrow 2}^2$	$\sigma_{3 \rightarrow 3}^3$	$\sigma_{100 \rightarrow 100}$
5	$\sigma_g - 1 \rightarrow g$	0	$\sigma_{1 \rightarrow 2}^1$	$\sigma_{2 \rightarrow 3}^2$	$\sigma_{99 \rightarrow 100}$
6	$\sigma_g - 2 \rightarrow g$	0	0	$\sigma_{1 \rightarrow 3}^1$	$\sigma_{98 \rightarrow 100}$
7	$\sigma_g - 3 \rightarrow g$	0	0	0	.
.	.	.	.	.	.
.	.	.	.	.	.
.	.	.	.	.	.
103	$\sigma_g - 99 \rightarrow g$	0	0	0	$\sigma_{1 \rightarrow 100}$

Table 2.3

DLC-2D Nuclei With Their Respective ID's - MAT ID  
Refers to the ID's on the Unformatted Library

ENDF/B ID	Material	MAT ID
1014	Mg	1 - 9
1017	V	10 - 27
1019	Mn-55	19 - 27
1026	Xe-135	28 (P <sub>o</sub> only)
1027	Sm-149	29 - 37
1028	Eu-151	38 - 46
1029	Eu-153	47 - 55
1030	Gd	56 - 64
1031	Dy-164	65 - 73
1032	Lu-175	74 - 82
1033	Lu-176	83 - 91
1043	U-234	92 - 100
1050	Pu-238	101 - 109
1056	Am-241	110 - 118
1057	Am-243	119 - 127
1060	W-182	128 - 136
1061	W-183	137 - 145
1062	W-184	146 - 154
1063	W-186	155 - 163
1083	Re-185	164 - 172
1084	Re-187	173 - 181
1085	Cu-63	182 - 190
1086	Cu-65	191 - 199
1087	Cu	200 - 208
1088	He	209 - 217
1105	Pu-240	218 - 226
1106	Pu-241	227 - 235
1111	Mo	236 - 244
1115	Li-6	245 - 253
1116	Li-7	254 - 262
1117	Th-232	263 - 271
1118	Co-59	272 - 280
1119	Pa-233	281 - 289
1120	D(H-2)	290 - 298
1121	Cr	299 - 307
1123	Ni	308 - 316
1126	Ta-181	317 - 325
1127	Ta-182	326 - 334
1133	N-14	335 - 343
1134	O-16	344 - 352
1135	Al-27	353 - 361

Table 2.3 Continued

---

ENDF/B ID	Material	MAT ID
1136	Pb	362 - 370
1138	Ag-107	371 - 379
1139	Ag-109	380 - 388
1141	Cs-133	389 - 397
1146	He-3	398 - 406
1148	H-1	407 - 415
1149	Cl	416 - 424
1150	K	425 - 433
1151	Si	434 - 442
1152	Ca	443 - 451
1154	Be-9	452 - 460
1155	B-10	461 - 469
1156	Na-23	470 - 478
1157	U-235	479 - 487
1158	U-238	488 - 496
1159	Pu-239	497 - 505
1160	B-11	506 - 514
1161	Pu-242	515 - 523
1162	Cm-244	524 - 532
1164	Nb-nat	533 - 541
1165	C-12	542 - 550
1166	Au-197	551 - 559
1180	Fe-nat	560 - 568

---

The unformatted library and MAT ID are defined in Chapter Three.

Table 2.4

Thermal Group Cross-sections for Nuclei  
Contained in the DLC-2D 100 Group  
Neutron Cross-section Library

$\sigma_a$	$v\sigma_f$	$\sigma_t$	$\sigma_s$	
0.294	0.0	52.124	51.83	H in H <sub>2</sub> O
4.61 E-4	0.0	3.350461	3.3500	D
0.0061	0.0	0.7299	0.7238	He
4721.0	0.0	4722.0	1.0	He-3
833.32	0.0	834.04	0.7200	L-16
3.1900E-2	0.0	1.0819	1.0500	L-17
0.00842	0.0	6.00842	6.0000	Be
3400.0	0.0	3402.2	2.20	B-10
0.00443	0.0	5.04043	5.0360	B-11
0.00298	0.0	4.73298	4.73	C
1.6785	0.0	11.6355	9.9570	N
1.60 E-4	0.0	3.70416	3.7040	O-16
0.4732	0.0	3.7932	3.32	Na
0.0549	0.0	3.4649	3.41	Mg
0.206	0.0	1.717	1.511	Al
0.1418	0.0	2.2918	2.15	Si
29.43	0.0	45.93	16.50	Cl
1.91	0.0	4.11	2.20	K
0.3833	0.0	2.9533	2.57	Ca
4.48	0.0	9.48	5.00	V
2.7473	0.0	7.0973	4.35	Cr
11.875	0.0	13.625	1.75	Mn
2.27	0.0	13.67	11.40	Fe
32.97	0.0	39.77	6.80	Co-59
4.0766	0.0	21.5766	17.50	Ni
3.36	0.0	11.06	7.70	Cu
3.986	0.0	9.564	5.578	Cu-63
1.95	0.0	17.37	15.42	Cu-65
1.0192	0.0	6.6792	5.66	Nb
2.35	0.0	7.35	5.00	Mo
32.61	0.0	39.01	6.40	Ag-107
81.53	0.0	86.53	5.00	Ag-109
2.34 E+6	0.0	2.64 E+6	3.00 E+5	Xe-135
26.14	0.0	33.24	7.10	Cs-133
54757.0	0.0	54922.0	165.0	Sm-149
7870.0	0.0	7873.4	3.40	Eu-151
381.07	0.0	385.83	4.76	Eu-153
36911.0	0.0	37081.0	170.0	Gd
2233.0	0.0	2622.0	389.0	Dy-164
22.94	0.0	28.21	5.27	Lu-175
1730.0	0.0	1733.0	3.00	Lu-176

Table 2.4 Continued

$\sigma_a$	$\nu\sigma_f$	$\sigma_t$	$\sigma_s$	
18.61	0.0	25.61	7.00	Ta-181
7310.0	0.0	7341.0	31.0	Ta-182
19.13	0.0	23.35	4.22	W-182
9.04	0.0	13.58	4.54	W-183
1.60	0.0	8.17	6.57	W-184
34.16	0.0	37.93	3.77	W-186
101.03	0.0	121.65	20.62	Re-185
66.29	0.0	76.39	10.10	Re-187
87.56	0.0	91.99	4.43	Au-197
0.158	0.0	11.352	11.194	Pb
6.56	0.0	18.38	11.82	Th-232
35.27	0.0	45.27	10.0	Pa-233
85.96	0.0	102.96	17.00	U-234
589.88	1222.2	605.66	15.78	U-235
2.41	0.0	11.36	8.95	U-238
498.76	39.70	519.44	20.68	Pu-238
964.98	2034.8	973.61	8.63	Pu-239
257.06	0.1481	260.79	3.73	Pu-240
1218.9	2621.0	1230.3	11.40	Pu-241
16.38	0.0	24.76	8.38	Pu-242
518.24	8.97	528.24	10.0	Am-241
159.52	0.0	169.52	10.0	Am-243
13.43	2.52	21.83	8.40	Cm-244

Table 2.5

Nuclei in DLC-2D 100-group Neutron  
Cross-section Library Requiring a  
Non-1/v Correction Factor at 293°K

---

Nuclide	Non-1/v factor at 293°K
Cd	1.3
Sm	1.5
Eu	0.95
Gd	0.85
Hg	0.95
U-235	0.981
Pu-239	1.075
U-nat	0.99

---



in nuclear systems with temperatures other than 293°K, one must use the appropriate temperature-dependent correction factors. The procedures involved in obtaining these values are discussed in reference 15, pages 251 to 256. Once the corrected thermal values are obtained, they can be re-entered in the appropriate cross-section table. This is a fairly simple task, because for a given nuclide one would need only to alter the  $P_0$  table entries and then only the values for thermal group. This correction can be accomplished by writing a small program that would retrieve, correct, and re-enter these values in the table or by modifying TAPE MAKER.

The conclusions to be drawn from the discussion of the DLC-2D cross-section data described in this section is that the usage of these cross-section sets is most appropriate when used in neutronic systems which contain fission sources and satisfy the assumption required for infinite dilution resonance correction. These systems then should have a neutron flux spectrum closely approximating the weighting spectrum, and must not contain any strong resonance absorber. The fission-source data<sup>(10)</sup> to be used with the DLC-2D cross-sections are included in Appendix A. The energy group structure is that of the DLC-2D library, and may be converted to broader-group spectra by simply summing over the desired few-group boundaries, since the values have been normalized.

## 2.2. DLC-37 100 Neutron-21 Gamma Group Cross-sections for EPR Neutronics

The DLC-37/EPR data set was generated at the Neutron Physics Division of ORNL. These cross-sections were produced for use in calculations involving fusion reactors, and in particular Tokamak Experimental Power Reactor (EPR) conceptual designs<sup>(11)</sup>. This library is also based on ENDF/B point cross-sections. The ENDF/B data were processed by selected modules<sup>(7)</sup> of the AMPX Modular System, to generate a coupled set of cross-sections for neutron and photon interactions. Neutron and photon-production cross-sections were weighted with a  $1/E$  function for  $E_n$  greater than 5 kT (0.345 MeV) and with a Maxwellian distribution peaked at 800°K for  $E_n$  equal to or less than 5 kT. The photon-interaction cross-sections were flat-weighted. All resonance nuclei were treated with infinite dilution approximation.

From the preceding discussion it is evident that the neutron-weighting spectrum for DLC-37/EPR data is quite different from that used in DLC-2D library. There is no fission spectrum present, and the weighting flux resembles that of neutron slowing down in fusion systems. Hence these data may be used for neutronics systems and attenuation problems satisfying these conditions, and where no strong resonance absorber exists.

The DLC-37 cross-sections also represents a  $P_0$  approximation to anisotropic elastic scattering. The neutron energy boundaries correspond to 14.918 MeV as group 1 and down to  $1.0 \times 10^{-4}$  eV as the limit of group 100. The remaining 21 groups constitute the gamma-ray

group structure with upper and lower energy limits at 14 and 0.01 MeV, respectively. Those group structures are tabulated in Tables 2.6A and 2.6B.

The EPR cross-sections were also generated for use in ANISN-formatted transport codes. They consist of one-dimensional fine-group constants  $\sigma_a$ ,  $\nu\sigma_f$ ,  $\sigma_t$ , and two-dimensional group-transfer matrices for neutron and gamma groups. In addition, activity cross-sections such as  $(n,t)$ ,  $(n,\alpha)$  are included for selected materials. The gamma cross-sections are tabulated in the same manner, except that group-transfer constants for scattering from a group less than 101 into a group greater than 100 represents photon production data. The neutron and gamma KERMA<sup>(12)</sup> (Kinetic Energy Released in Material) factors are also included in the library for some nuclei. The term KERMA factor refers to the energy released in the material and is specified such that the heat produced at that energy can be obtained merely by multiplying by the energy-dependent flux. Symbolically this can be represented as:

$$H_n(\bar{r}, E_n) = \sum_j N_j(\bar{r}) \phi_n(\bar{r}, E_n) K_{nj}(E_n)$$

$$H_\gamma(\bar{r}, E_\gamma) = \sum_j N_j(\bar{r}) \phi_\gamma(\bar{r}, E_\gamma) K_{\gamma j}(E_\gamma)$$

$$K_{nj}(E) = \sum_i \sigma_{ij}(E) E_{ij}(E)$$

$$K_{\gamma j}(E) = \sum_i \sigma_{ij}(E) E_{ij}(E)$$

with  $i$  representing a reaction and  $j$  an element.

$\bar{r}$  = denotes spatial variables

$H_n(\bar{r}, E_n)$  = energy-dependent neutron heating

$H_\gamma(\bar{r}, E_\gamma)$  = energy-dependent gamma heating

$K_{nj}(E_n)$  = neutron KERMA factor for element j and  
incident energy  $E_n$

$K_{\gamma j}(E_\gamma)$  = gamma KERMA factor for element j and incident  
energy  $E_\gamma$

$N_j$  = number of atoms of element j per  $\text{cm}^3$

$\phi_n/\phi_\gamma$  = neutron/gamma energy-dependent flux

$\sigma_{ij}(E)$  = microscopic cross-section of element j for  
reaction i at energy E

$E_{ij}(E)$  = energy deposited per reaction i in element j.

Note that the  $K_{nj}$  and  $K_{\gamma j}$  denote microscopic KERMA factors as defined above. Hence, the total nuclear heating  $H_t(\bar{r})$  at position  $\bar{r}$  is defined as:

$$H_t(\bar{r}) = \int H_n(\bar{r}, E_n) dE_n + \int H_\gamma(\bar{r}, E_\gamma) dE_\gamma$$

The DLC-37/EPR library contains these microscopic KERMA factors. When utilizing them, one should note that these KERMA factors are treated as activity cross-sections. This means they are multiplied

by the number density  $N_j$  (as specified by the user) to produce macroscopic KERMA factors, and by the flux to produce neutron and gamma heating terms in the material.

The DLC-37/EPR library members are listed in Table 2.7, along with the ENDF/B ID's, MAT ID's, and some remarks concerning the data. Table 2.8 represents the coupled 121-group data organization in a matrix form. The table positions occupied by the group constants are the same as those in DLC-2D library for neutrons. As shown in the table, in case of gamma cross-sections, there are also production terms, as indicated before.

Table 2.6A

## DLC-37/EPR 100-group Neutron Multigroup Structure

Group	Energy Range (eV)		Group	Energy Range (eV)	
1	1.4918E 07*	1.3499E 07	51	8.6517E 04	6.7380E 04
2	1.3499E 07	1.2214E 07	52	6.7380E 04	5.2475E 04
3	1.2214E 07	1.1052E 07	53	5.2475E 04	4.0868E 04
4	1.1052E 07	1.0000E 07	54	4.0868E 04	3.1828E 04
5	1.0000E 07	9.0484E 06	55	3.1828E 04	2.4788E 04
6	9.0484E 06	8.1873E 06	56	2.4788E 04	1.9305E 04
7	8.1873E 06	7.4082E 06	57	1.9305E 04	1.5034E 04
8	7.4082E 06	6.7032E 06	58	1.5034E 04	1.1709E 04
9	6.7032E 06	6.0653E 06	59	1.1709E 04	9.1188E 03
10	6.0653E 06	5.4881E 06	60	9.1188E 03	7.1018E 03
11	5.4881E 06	4.9659E 06	61	7.1018E 03	5.5309E 03
12	4.9659E 06	4.4933E 06	62	5.5309E 03	4.3074E 03
13	4.4933E 06	4.0657E 06	63	4.3074E 03	3.3546E 03
14	4.0657E 06	3.6788E 06	64	3.3546E 03	2.6126E 03
15	3.6788E 06	3.3287E 06	65	2.6126E 03	2.0347E 03
16	3.3287E 06	3.0119E 06	66	2.0347E 03	1.5846E 03
17	3.0119E 06	2.7253E 06	67	1.5846E 03	1.2341E 03
18	2.7253E 06	2.4660E 06	68	1.2341E 03	9.6112E 02
19	2.4660E 06	2.2313E 06	69	9.6112E 02	7.4852E 02
20	2.2313E 06	2.0190E 06	70	7.4852E 02	5.8295E 02
21	2.0190E 06	1.8268E 06	71	5.8295E 02	4.5400E 02
22	1.8268E 06	1.6530E 06	72	4.5400E 02	3.5358E 02
23	1.6530E 06	1.4957E 06	73	3.5358E 02	2.7537E 02
24	1.4957E 06	1.3534E 06	74	2.7537E 02	2.1445E 02
25	1.3534E 06	1.2246E 06	75	2.1445E 02	1.6702E 02
26	1.2246E 06	1.1080E 06	76	1.6702E 02	1.3007E 02
27	1.1080E 06	1.0026E 06	77	1.3007E 02	1.0130E 02
28	1.0026E 06	9.9718E 05	78	1.0130E 02	7.8893E 01
29	9.0718E 05	8.2085E 05	79	7.8893E 01	6.1442E 01
30	8.2085E 05	7.4274E 05	80	6.1442E 01	4.7851E 01
31	7.4274E 05	6.7206E 05	81	4.7851E 01	3.7267E 01
32	6.7206E 05	6.0810E 05	82	3.7267E 01	2.9023E 01
33	6.0810E 05	5.5023E 05	83	2.9023E 01	2.2603E 01
34	5.5023E 05	4.9787E 05	84	2.2603E 01	1.7604E 01
35	4.9787E 05	4.5049E 05	85	1.7604E 01	1.3710E 01
36	4.5049E 05	4.0762E 05	86	1.3710E 01	1.0677E 01
37	4.0762E 05	3.6883E 05	87	1.0677E 01	8.3153E 00
38	3.6883E 05	3.3373E 05	88	8.3153E 00	6.4760E 00
39	3.3373E 05	3.0197E 05	89	6.4760E 00	5.0435E 00
40	3.0197E 05	2.7324E 05	90	5.0435E 00	3.9279E 00

\* Read 1.4918 x 10<sup>7</sup>

Table 2.6A Continued

---

Group	Energy Range (eV)		Group	Energy Range (eV)	
41	2.7324E 05	2.4724E 05	91	3.9279E 00	3.0590E 00
42	2.4724E 05	2.2371E 05	92	3.0590E 00	2.3824E 00
43	2.2371E 05	2.0242E 05	93	2.3824E 00	1.8554E 00
44	2.0242E 05	1.8316E 05	94	1.8554E 00	1.4450E 00
45	1.8316E 05	1.6573E 05	95	1.4450E 00	1.1254E 00
46	1.6473E 05	1.4996E 05	96	1.1254E 00	8.7644E 01
47	1.4996E 05	1.3569E 05	97	8.7644E 01	6.8257E 01
48	1.3569E 05	1.2277E 05	98	6.8257E 01	5.3159E 01
49	1.2277E 05	1.1109E 05	99	5.3159E 01	4.1400E 01
50	1.1109E 05	8.6517E 04	100	4.1400E 01	1.0000E 04

---

Table 2.6B  
 DLC-37/EPR 21-group Gamma Multigroup Structure

Gamma-ray Group	Coupled Group	Group Boundaries (MeV)
1	101	1.2E01 - 1.4E01*
2	102	1.0E01 - 1.2E01
3	103	8.0E00 - 1.0E01
4	104	7.5E00 - 8.0E00
5	105	7.0E00 - 7.5E00
6	106	6.5E00 - 7.0E00
7	107	6.0E00 - 6.5E00
8	108	5.5E00 - 6.0E00
9	109	5.0E00 - 5.5E00
10	110	4.5E00 - 5.0E00
11	111	4.0E00 - 4.5E00
12	112	3.5E00 - 4.0E00
13	113	3.0E00 - 3.5E00
14	114	2.5E00 - 3.0E00
15	115	2.0E00 - 2.5E00
16	116	1.5E00 - 2.0E00
17	117	1.0E00 - 1.5E00
18	118	4.0E-01 - 1.0E00
19	119	2.0E-01 - 4.0E-01
20	120	1.0E-01 - 2.0E-01
21	121	1.0E-02 - 1.0E-01

\* Read  $1.4 \times 10^1$ .



Table 2.7

DLC-37/EPR Nuclei with Their ID's - MAT ID Refers to ID's on the Unformatted Tape

MAT ID	Material	ENDF/B ID	Remarks
1 - 9	Ni	1190	
10 - 18	Cr	1191	
19 - 27	Fe	1192	
28 - 36	Mn-55	1197	
37 - 45	Co-59	1199	
46 - 54	Cu	1295	
55 - 63	He-4	1270	No $\gamma$ production data
64 - 72	C	1274	
73 - 81	O	1276	
82 - 90	Al	1193	
91 - 99	Pb	1288	
100 - 108	Li-6	1271	
109 - 117	Li-7	1272	
118 - 126	B-10	1273	
127 - 135	H	1269	Water bound thermal n x-sec ( $\sigma_S = 45b, \sigma_{n,\gamma} = 0.18b$ )
136 - 144	Be-9	1289	
145 - 153	V	1196	
154 - 162	Nb	1164	
163 - 171	B-11	1160	
172 - 180	Li	1286	
181 - 189	F	1277	
190 - 198	Si	1194	
199 - 207	Mg	1280	
208 - 216	K	1150	
217 - 225	Na	1156	No $\gamma$ production data

Table 2.7 Continued

MAT ID	Material	ENDF/B ID	Remarks
226 - 234	N	1275	
235 - 243	Mo	1287	
244 - 252	Zr-nat	7141	
253 - 261	U-235	1261	
262 - 270	U-238	1262	
271 - 279	P-31	7121	
280 - 288	S-32	7122	
289 - 297	Sn	7150	
298 - 306	Cl	1149	
307 - 315	Ca	1195	
336	B-10(n,t)2alpha		(n,t)2α x-sec in Position 1; zeros elsewhere
337	B-10(n,alpha)		(n,α) x-sec in Position 1; zeros elsewhere
338	B-11(n,t)		
339	B-11(n,alpha)		(n,α) x-sec in Position 1; zeros elsewhere
340	Li-6(n,t)		(n,t) x-sec in Position 1; zeros elsewhere
341	Li-7(n,n't)		(n,n't) x-sec in Position 1; zeros elsewhere
342	Li-6(n,t) hot		(n,t) x-sec in Position 1; zeros elsewhere
343	Kerma Factors		
344 - 352	Nb	1189	
353 - 361	Np-237	1263	
362 - 370	Pu-239	1264	
371 - 379	Au-197	4283(M1)	
380 - 388	W-182	4582(M3)	No γ production data
389 - 397	W-183(M4)		No γ production data
398 - 406	W-184	4584(M4)	No γ production data

Table 2.7 Continued

MAT ID	Material	ENDF/B ID	Remarks
407 - 415	W-186	4586(M3)	No $\gamma$ production data
416 - 424	Ta-181	1285	
425 - 433	Th-232	1296	
434 - 442	U-233	1260	

The unformatted tape and MAT ID are defined in Chapter Three.

Table 2.8

Data Organization of EPR Cross-section, Illustrating Table Position, Cross-section Type, and Neutron Energy Groups

Position	x-sec Type	Groups:g									
		1	2	3		100	101	102	103		121
1	$\sigma_a$	$\sigma_n^1$	$\sigma_n^2$	$\sigma_n^3$	.	$\sigma_n^{100}$	$\sigma_n^1$	$\sigma_n^2$	$\sigma_n^3$	.	$\sigma_n^{21}$
2	$\nu\sigma_f$	$\sigma_n^1$	$\sigma_n^2$	$\sigma_n^3$	.	$\sigma_n^{100}$	0	0	0	.	0
3	$\sigma_t$	$\sigma_n^1$	$\sigma_n^2$	$\sigma_n^3$	.	$\sigma_n^{100}$	$\sigma_n^1$	$\sigma_n^2$	$\sigma_n^3$	.	$\sigma_n^{21}$
4	$\sigma_s \rightarrow s$	$s_n^1$	$s_n^2$	$s_n^3$	.	$s_n^{100}$	$s_n^1$	$s_n^2$	$s_n^3$	.	$s_n^{21}$
5	$\sigma_{g-1 \rightarrow g}$	0	$s_n^2$	$s_n^3$	.	$s_n^{100}$	$p_n^1$	$s_n^2$	$s_n^3$	.	$s_n^{21}$
6	$\sigma_{g-2 \rightarrow g}$	0	0	$s_n^3$	.	$s_n^{100}$	$p_n^1$	$p_n^2$	$s_n^3$	.	$s_n^{21}$
7	$\sigma_{g-3 \rightarrow g}$	0	0	0	.	$s_n^{100}$	$p_n^1$	$p_n^2$	$p_n^3$	.	$s_n^{21}$
.	.	.	.	.	.	.	.	.	.	.	.
.	.	.	.	.	.	.	.	.	.	.	.
.	.	.	.	.	.	.	.	.	.	.	.
124	$\sigma_{g-120 \rightarrow g}$	0	0	0	.	0	0	0	0	.	$p_n^{21}$

n = indicates neutron cross-section,  $\gamma$  = indicates photon cross-sections, s = indicates scattering cross sections and p = indicates production cross-sections.

## CHAPTER THREE

### Data Retrieval from Master Cross-section Libraries

The fine-group libraries described in the previous chapter are organized in a format suitable for use with ANISN-formatted multigroup transport or probabilistic codes. Examples of these computer programs are ANISN<sup>(1)</sup> and DOT<sup>(13)</sup> multigroup discrete-ordinates transport codes in one and two-dimensional geometries, respectively, and the Monte Carlo probabilistic code, MORSE<sup>(14)</sup>. Before proceeding with cross-section retrieval schemes, it is necessary to describe this data organization. An ANISN formatted cross-section library consists of tables of data for each group,  $g$ , of each material in the following manner:

<u>Table Position</u>	<u>Cross-section Type</u>
1	activity
.	.
.	.
.	.
IHT-2	absorption
IHT-1	$\nu$ * fission
IHT	total
IHT+1	$\sigma_{g+NUS \rightarrow g}$
.	.
.	.
.	.
IHS-1	$\sigma_{g+1 \rightarrow g}$
IHS	$\sigma_{g \rightarrow g}$
IHS+1	$\sigma_{g-1 \rightarrow g}$
.	.
.	.
.	.
IHM	$\sigma_{g-NOS \rightarrow g}$

---

NUS is the number of groups of upscatter for neutrons that gain energy while scattered. NDS is the number of groups of downscatter. IHT, IHS, and IHM refer to the positions of  $\sigma_t$ ,  $\sigma_{g \rightarrow g}$  (within-group scattering), and cross-section table length, respectively. Hence, upscatter data are in positions IHT+1 to IHS-1, and positions IHS+1 to IHM are used for downscatter values. If there are no activity cross-sections, IHT = 3. If there is no upscatter then IHS = IHT+1; and in a one-group problem (i.e., no downscatter), IHM = IHS. The term "material" as used here refers to each  $P_0$  component, and the  $P_\ell$  cross-section tables correspond in format to the  $P_0$  tables, even though the transfer coefficients are the only values used. For the DLC-2D data, IHT = 3, IHS = 4, and IHM = 103. For the DLC-37/EPR library, we have IHT = 3, IHS = 4, and IHM = 124.

The master cross-section libraries are written on magnetic tape in BCD (Binary Coded Decimal) Card-image format. These data must be retrieved and re-written in unformatted and compiled versions. This secondary library tape is called an ANISN Binary Tape (ABT), or an ANISN unformatted tape. The ABT is then the input cross-section library to the transport codes.

Creating the ABT's for DLC-2D and DLC-37/EPR is facilitated through use of the computer programs LIBGEN<sup>(7)</sup> and LIBGEN2. The code LIBGEN was supplied in the DLC-37/EPR code package by Radiation Shielding Information Center, and is used with EPR cross-sections. The code LIBGEN2 was written at LSU to convert the DLC-2D data, and represents a modification to LIBGEN. The generated master libraries

were then named "DLC37D.UNFORM" and "DLC2D.UNFORM", respectively. Each material in these cross-section libraries is identified with a unique ID number. These ID numbers were listed in Tables 2.3 and 2.6 as "MAT ID" for each library.

The binary fine-group cross-sections can now be directly input to the multigroup transport codes that use the ANISN format, or they may be modified further to satisfy the input requirements of other codes. Future discussions in this thesis are limited to ANISN-formatted input.

## CHAPTER FOUR

### Collapsing the Fine-group Cross-sections into Broader Groups

#### 4.1. Preliminary Considerations

As indicated in the discussion of selecting data from cross-section libraries, once a binary tape is created, it can be used in multigroup calculations. This in principle would provide the user with a many-group treatment of the problem.

However, in many computer installations the amount of the storage locations needed in the core would prevent such fine-group calculations. This may be illustrated by noting that for one material (i.e., one  $P_g$  value) in the DLC-2D library, there are 100 by 103, or 10300, entries in the cross-section table. Since each number requires one location (four bytes) to be stored, for each  $P_g$  value the amount of the required core becomes 100 by 103 by 4 bytes. In terms of the more familiar unit K, which is 1024 bytes, the required storage becomes approximately 40 k. Therefore, in a problem involving five nuclides and a  $P_g$  approximation, one would need about 5 by 9 by 40 k = 1800 k, just to store the cross-sections in the core. Considering the additional amount of core necessary to do the calculations, this number soon becomes too great to be readily available to the user. In addition, the required amount of the Central Processing Unit (CPU) time becomes too excessive to justify such calculations.



To cope with these difficulties, one must use a lower order of  $P_\ell$  approximation and a smaller number of energy groups in multi-group calculations. Usually a choice of low order expansion of elastic scattering angular distributions does not imply a significant inaccuracy in the results (see Section 5.4 of Ref. 16). For majority of problems, a  $P_3$  approximation is sufficient. In problems dealing with a large number of nuclei and mesh spacings, one may even choose lower orders of  $P_\ell$  to reduce the required memory and CPU time. A detailed discussion of the adequacy of the order of  $P_\ell$  and the discrete ordinates methods is given in Chapter 5 of reference 16. The critical problem then becomes that of reducing the number of energy groups by collapsing the fine-group data into broader energy groups. Again, the assumption is made that using a smaller group structure would not disturb the accuracy of the results significantly<sup>(18)</sup>.

As mentioned before, an adequate set of cross-sections must be chosen for a given problem prior to collapsing. The next step would be to determine the group boundaries for the desired few-group structure. The governing rule lies within the concept of lethargy and the amount of detail desired in the computed neutron flux spectrum for the system. Since the average number of collisions a neutron experiences per unit lethargy while slowing down is constant, the most accurate group constants are generated by using energy group spacing of equal lethargy width. Thus, the fine-group members are collected together such that the lethargy width of the resulting

broad-group remains constant. However, if it is desired to obtain a detailed spectrum in a certain energy range, a finer group spacing (or a larger number of broad groups) would be used in that energy range. A combination of the above two categories would then determine the energy boundaries for the few-group structure. As an example, for a given problem one may choose a lethargy spacing of 1.0 for the first few broad groups and a spacing of 2.5 for the remaining broad groups.

The preliminary steps discussed above must be taken before the actual collapsing calculations are performed. Once the fine-group cross-section library is selected, the few-group boundaries chosen, and a  $P_0$  value is determined, an appropriate computer code is used to collapse the data.

#### 4.2. APRFX-I Code

APRFX-I is used to collapse the DLC-2D fine-group cross-sections into a broader-group structure according to a flux spectrum either input by the user or calculated by the code. The code will average the fine-group data to form either macroscopic or microscopic nuclide cross-sections and any combination of macroscopic mixtures of these cross-sections. This program also determines the broad-group input source and generates neutron velocities from the formula:

$$v = c \sqrt{1 - \frac{m_0 c^2}{T + m_0 c^2}}$$

where  $m_0$  is the neutron rest mass,  $c$  is the speed of light in vacuum, and  $T$  is the neutron average kinetic energy.

The flux calculation performed by APRFX-I is a solution to the multigroup diffusion equation which provides an estimate of the fine-group spectrum. The form of the diffusion equation utilized in the code is,

$$[D_i B^2 + \Sigma_a^i + \sum_{h>i}^N \Sigma(i \rightarrow h)] \phi_i = \sum_{h=1}^{i-1} \Sigma(h \rightarrow i) \phi_h + v \Sigma_{fi} \phi_i + X_i.$$

where a  $DB^2$  leakage term is used to account for the usual dimensional diffusion leakage term. The terms have the definitions:

$D_i$  = diffusion coefficient for group  $i$

$B^2$  = buckling factor

$\Sigma_a^i$  = absorption cross section for group  $i$

$\Sigma(i \rightarrow h)$  = scattering matrix element for transfer from group  $i$  to group  $h$ .

$X_i$  = fraction of source neutrons in group  $i$  (fission or extraneous)

$v \Sigma_{fi}$  = (neutrons/fission) x fission cross section for group  $i$

$\phi_i$  = flux for group  $i$

The code solves for the group fluxes beginning with the highest energy group and continuing through the sink group. The fluxes are normalized

by

$$\sum_{i=1}^N \phi_i = 1.$$

The code assumes a homogenous medium, and a so-called  $DB^2$  leakage term<sup>(18)</sup> is used to account for the dimensional diffusion leakage. The geometry of the system is taken into account by inputting the buckling factor  $B^2$ , which relates to the system via the reactor equation  $\nabla_r^2 \phi_T(r) + B^2 \phi_T(r) = 0$ <sup>(29)</sup>. The buckling is a measure of the thermal flux curvature in the system and varies inversely with the size of the system. This may be seen from solving the reactor equation for  $B^2$ :  $B^2 = -\nabla^2 \phi_T(r) / \phi_T(r)$ . The diffusion coefficient,  $D$ , is defined as  $1/3\Sigma_{tr}$  with  $\Sigma_{tr}$  being the transport cross section<sup>(19)</sup>. The transport cross section is determined from the scattering cross section by  $\Sigma_{tr} = \Sigma_s(1 - \bar{\mu}_0)$ , where  $\bar{\mu}_0$  is the cosine of the average angle of scatter in the laboratory system. For any scattering nuclide of mass  $A$ ,  $\bar{\mu}_0 = 2/3A$ .

Reference 2 provides a description of the input parameters and the different options available with APRFX-I. The code was slightly modified at LSU by the author by addition of an auxiliary routine, subroutine IMAGE, to produce a card image listing of the input data. Since APRFX-I was written for use with the DLC-2D library, the fine-group cross-sections are directly inputted to the code in BCD form rather than the DLC2D.UNIFORM library.

From the assumptions made in APRFX-I, it is evident that the code is most appropriate for use with homogenous media and systems that can be accurately described by diffusion theory. The results

will not be as accurate as those obtained from ANISN<sup>(24)</sup>, which uses the discrete-ordinates transport-theory solution to the generalized Boltzmann equation and is capable of a more accurate modeling of the various regions and geometry of the system. Wyatt<sup>(24)</sup> points out that the APRFX-I code itself may contain inaccuracies.

APRFX-I is retained on magnetic tape T2140 at LSU; it can be accessed by the following Data Definition (DD) statement.

```
//FORT.SYSIN DD UNIT=TAPE, VOL=SER=T2140,
//          DSN='APRFX-I.IMAGE', LABEL=9, DISP=OLD.
```

An example problem is outlined in Figure 4.1. The JCL commands and input data required to treat this problem are given as Figure 4.2.

The density factors are calculated according to  $\rho \frac{N_A}{A} * 10^{-24}$  to obtain atoms/barn-cm where:

$\rho$  = density of material in the mixture,

$N_A$  = Avogadro's number, and

A = atomic mass of the material

The mixing table (DIFM, DAVE, DF entries) is not used, and the actual mixture densities are entered for the parameter DAVE. The complete listing of the input cards is given in Figure 4.2. The input data are actually used twice: The MAIN program calls IMAGE to produce a listing of the input data in the first step, then the data is read again for use by the other subroutines. This requires rewinding the Logical Unit 5 (FT05F001). Hence the input data are initially placed on a temporary disk space, since the card-reader cannot be rewound.

Figure 4.1

## Example of APRFX-I Collapsing

Assume a cylindrical reactor of dimensions  $R = 180$  cm and  $H = 168$  cm with three regions composed of:

<u>Material</u>	<u>Region 1</u>		<u>Region 2</u>		<u>Region 3</u>	
Fe	5.566	gr/cc	7.87	gr/cc	0.0	gr/cc
C	0.0	gr/cc	0.0		1.536	gr/cc
U-235	$3.954 \times 10^{-3}$	gr/cc	0.0		$3.045 \times 10^{-3}$	gr/cc

It is desired to collapse the mixture cross-sections into 27 groups, given the fission spectrum of U-235 and a  $P_0$  expansion.



Figure 4.2 (continued)

```
//STEP2 EXEC FORTGCLG, REGION=200K, TIME=10
//FORT.SYSIN DD UNIT=TAPE, VOL=SER=T2140,
// DSN='APRFX-I. IMAGE', LABEL=9, DISP=OLD
//GO.FT01F001 DD UNIT=TAPE, VOL=SER=T1522,
// LABEL=15, DISP=OLD, DSN='100G.X-SEC.LIB'
//GO.FT03F001 DD UNIT=SYSDA, SPACE=(CYL,(10,10),RLSE),
// DCB=(RECFM=VBS, LRECL=80, BIKSIZE=3200)
//GO.FT02F001 DD DUMMY
//GO.SYSIN DD UNIT=SYSDA, SPACE=(TRK,(10,10),RLSE),
// DSN='DUMY.DATA', DISP=(OLD,DELETE)
//
```



This is indicated by STEP 1 in Figure 4.2, where the utility program COPYSOUT<sup>(21)</sup> is used. SYSUT2 specifies the output allocation to a temporary disk space, and SYSUT1 refers to the input data. STEP 2 indicates execution of the APRFX-I program.

A partial listing of the output is included in Appendix B. Often it is more convenient to store the collapsed cross sections on a tape file. This option is invoked by specifying ISPC greater than one and the DD statement in Figure 4.3. The output is written on Logical Unit N6 = 2 (FT02F001).

#### 4.3. ANISN Code

A detailed discussion of the historical background and the numerical methods incorporated in ANISN code is given in Reference 1. ANISN uses a multigroup discrete-ordinates method with general anisotropic scattering to solve deep penetration problems. The code can be used to solve the one-dimensional Boltzmann Transport Equation for neutrons or gamma rays in slab, sphere, or cylindrical geometry.

ANISN can also be used to collapse fine-group cross-section sets into few-group structures. The code calculates the weighting-fluxes according to source specification and medium configuration as input by the user. The cross sections are collapsed and then used in the next ANISN run for few-group calculations.

The most convenient way of using ANISN is to collapse the data, store the results on a temporary direct-access device (disk) and then perform the desired calculations on the same job step. This is easily done since ANISN allows multiple cases on the same job step. The ANISN Binary Tape (ABT) can be directly input to the code,

Figure 4.3

## Allocation of Tape Output for APRFX-I

```
//GO.FT02F001 DD UNIT=TAPE, LABEL=j, DSN=data set name,  
//              VOL=SER=T___, DISP=(NEW,KEEP)
```

where j = file number

T\_\_\_ = a "T" followed by a four digit tape number for the  
output tape which should contain the collapsed  
cross-sections.

This card replaces the previous DUMMY Card, //GO.FT02F001 DD DUMMY,  
in Figure 4.2.

and ANISN will mix the cross section sets to form macroscopic mixture cross sections. The activity cross sections and upscatter data may also be input. ANISN can compute activities for mixtures for a given region or interval. A total upscatter cross-section for each group of each material would also be calculated and placed in cross-section table position IHM+1 as discussed in Chapter Three, if so desired.

In most ANISN collapsing problems, one deals with several different elements. As discussed in the beginning of this chapter, a very large amount of computer core would be required for these cases. This problem can be overcome by using an auxiliary code TAPE MAKER<sup>(8)</sup>. This code retrieves the cross sections from an ABT library and, after rearranging the data, writes a group independent tape (GIT). When the GIT is used with ANISN, rather than storing the entire matrix, only the cross-sections for a single group are stored in the memory while the calculations for that group are performed. Data for the next group then replaces the previous cross-section sets before calculations for that group are performed. When the GIT option is used, only the mixture cross sections are saved and written on tape. It should be noted that since TAPE MAKER calculates the macroscopic mixture cross sections, the mixing table (10S, 11S, 12 \* entries) is eliminated from the ANISN card input data.

In order to make TAPE MAKER operable at LSU on the IBM 360/65 computer, the code was modified by the author by allocation of low speed core as well as high speed core. This is explained briefly in Appendix C. The TAPE MAKER program is on tape T2140 and

can be retrieved by the following DD card:

```
//FORT.SYSIN DD UNIT=TAPE, VOL=SER=T2140  
//          DSN='TAPE.MAKER', LABEL=11, DISP=OLD.
```

In order to facilitate the preparation and the correction of the input data for ANISN and TAPE MAKER, two other codes were developed by the author. These programs were primarily constructed from the subroutines in ANISN and TAPE MAKER codes which read the input data, check for the discrepancies, and write error messages. Hence they were called ANISN.SCANNER and T.M.TEST. Both of these codes include the auxiliary subroutine IMAGE which produces a card image listing of the input data. The usefulness of these scanning programs would be apparent if one notices that typical running times for ANISN.SCANNER and T.M.TEST are about two minutes and ten seconds, respectively. The corresponding ANISN and TAPE MAKER jobs would require about 30 minutes and two minutes CPU time, respectively. Once the card input and the cross-section data are checked to be correct, the execution of the corresponding ANISN or TAPE MAKER case is almost inevitable.

Some details of the preparation of the ANISN code may be in order. ANISN consists of several subroutines and uses the OVERLAY feature of the IBM Systems 360 Linkage Editor<sup>(20, 21, 22)</sup>. This means a particular set of subroutines are compiled at a time and then linked together to be loaded for execution in the form of a Load Module<sup>(23)</sup>. The compiled version of a program is called an Object Module to the Linkage Editor. This process requires about five minutes CPU-time in each ANISN case. It is possible to store

the Load Module of ANISN permanently and as a Cataloged Data Set<sup>(25)</sup>, to avoid wasting time. Hence, a Load Module of ANISN was created by the author and cataloged on disk. This procedure is often necessary when setting up large computer codes at an installation. Since a detailed description of this procedure may be of value in other applications, it has been included in Appendix D along with the required JCL cards.

When using the multigroup transport codes ANISN, DOT, or MORSE, the user should consult the Supplementary User's Manuals for these codes. These manuals were produced at the LSU Nuclear Science Center as parts of M. S. theses of other students<sup>(26, 27, 28)</sup>.

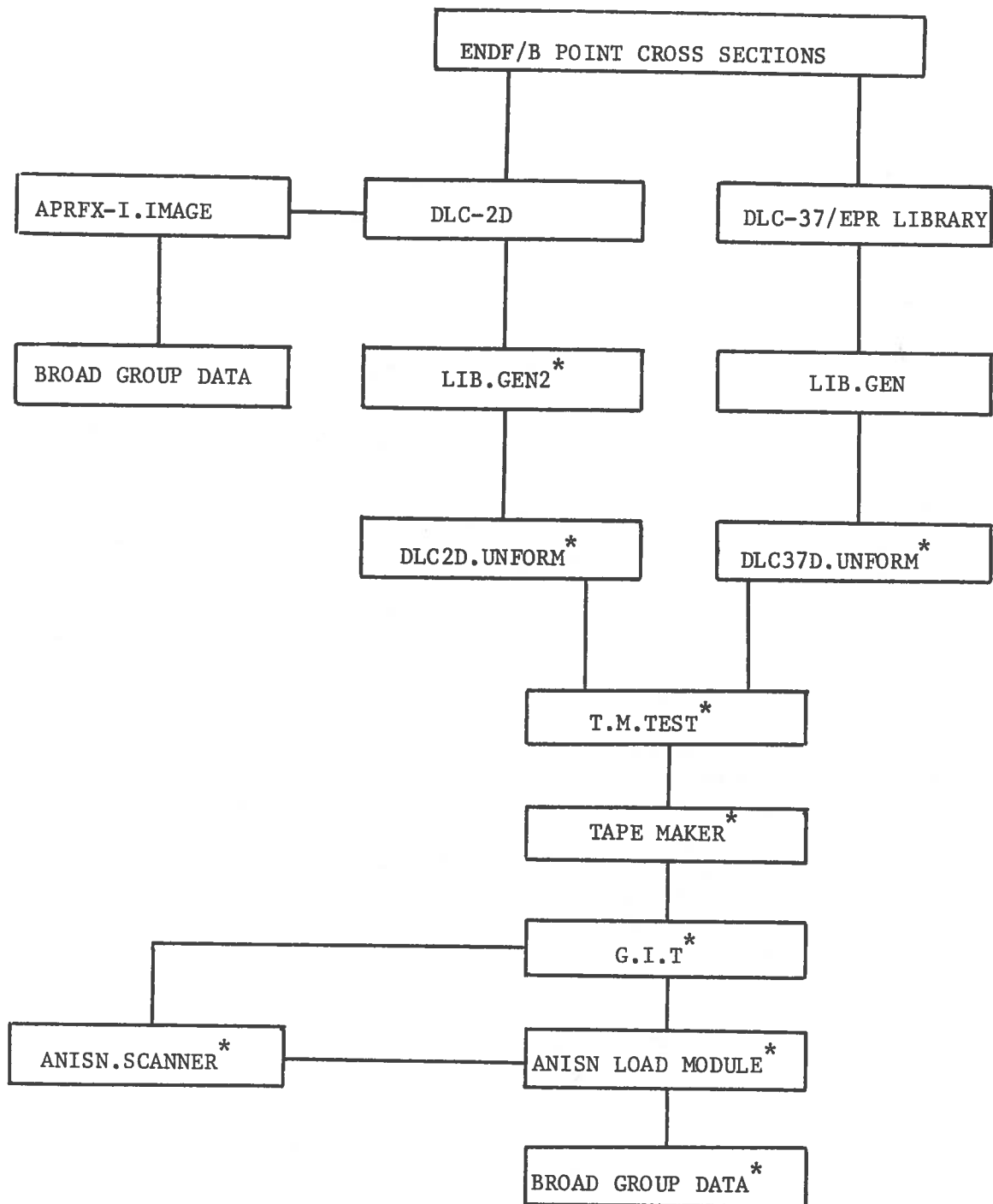
ANISN-collapsing example problems are presented in the following section. These example cases are categorized as DLC-2D Applications and DLC-37/EPR Applications. A general approach to the collapsing of fine-group data is indicated in Figure 4.4. The computer codes and data sets that were created or modified to be operable at LSU by the author are designated by an asterisk (\*).

#### 4.4. DLC-2D Applications

Consider the problem outlined in Figure 4.1. An ANISN-P<sub>0</sub> calculation is performed with and without using the GIT to compare the number of locations required to store the cross sections. The input to TAPE MAKER is shown in Figure 4.5. The ANISN.SCANNER JCL cards are listed in Figure 4.6, while the results for both runs are shown in Figures 4.7A and 4.7B. As it can be seen, the number of locations is greatly reduced when using the GIT option for cross sections.

Figure 4.4

Broad Group Data Preparation for  
Multigroup Transport Codes



\* Indicates codes were modified or created by the author.

Figure 4.5

Input to TAPE MAKER for P<sub>0</sub> Treatment of Cylindrical Reactor of Figure 4.1

```

//TMAKERPO JOB (260,7011,2), '44560 FARHUD'
//*SETUP T1929,T1927,T2140
//STEP1 EXEC PGM=COPY SOUT
//SYSUT2 DD UNIT=SYS DA,SPACE=(CYL,(2,1),RLSE),
DISP=(NEW,PASS),DSN='DUMB.DAYA'
//SYSUT1 DD *
50000
100 3 4 103 8 0 3 3 0 2 5
10$ 4 2R 5 3R 5
11$ 0 0 1 1 3 3
12$ 0.0 5- 1.0129 2- 5.9970 0.0 2- 8.4790
13$ 0.0 6- 7.8000 2- 7.6980 542 560
T 479
// EXEC FORTGCLG,PARM,FORT='MAP',
// PARM.LKED='XREF,LIST,MAP,HIAR',
// TIME=15,REGION=(260K,200K)
//FORT.SYS PRINT DD DUMMY,SY SOUT=
//FORT.SYS IN DD DSN='TAPE.MAKER',UNIT=TAPE,LABEL=11,
// VOL=SER=T2140,DISP=OLD
//LKED.SYS IN DD *
HIARCHY 1,AAA
ENTRY MAIN
//GO.FT01F001 DD UNIT=SYS DA,SPACE=(CYL,(10,10),RLSE),
// DCB=(RECFM=VBS,LRECL=80,BLKSIZE=3200)
//GO.FT02F001 DD UNIT=SYS DA,SPACE=(CYL,(10,10),RLSE),
// DCB=(RECFM=VBS,LRECL=80,BLKSIZE=3200)

```

Figure 4.5 (continued)

```
//GO.FT04F001 DD UNIT=SYSDA,SPACE=(CYL,(10,10),RLSE),
//   DCB=(RECFM=VBS,LRECL=80,BLKSIZE=3200)
//GO.FT08F001 DD UNIT=TAPE,VOL=(,RETAIN,SER=T1927,
//   LABEL=4,DSN=GITPO,DISP=(NEW,PASS),
//   DCB=(RECFM=VBS,LRECL=80,BLKSIZE=3200)
//GO.FT09F001 DD UNIT=TAPE,DSN='DIC2D.UNFORM',LABEL=1,
//   VOL=SER=T1929,DISP=OLD
//GO.SYSIN DD UNIT=SYSDA,SPACE=(TRK,(10,10)),
//   DSN='DUMY.DATA',DISP=(OLD,DELETE)
//   EXEC TAPEMAP,VOL=T1927
```



Figure 4.6

ANISN . SCANNER JCL Cards

```
//SCANPO JOB (260,7011,2,1),44560 FARHUD'  
/*SETUP T2140,T1927  
//STEP1 EXEC EGM=COPY SOUT  
//SYSUT2 DD UNIT=SYSDA,SPACE=(TRK,(10,10)),  
// DISP=(NEW,PASS),DSN='DUMY.DATA'  
//SYSUT1 DD *  
  
***** INPUT DATA *****  
  
//STEP2 EXEC FORTGCLG,REGION=260K,TIME=5  
//FORT.SYSRINT DD DUMMY,SY SOUT=  
//FORT.SYSIN DD UNIT=TAPE,VOL=SER=T2140,DSN='ANISN.SCANNER',  
LABEL=8,DISP=OLD  
//LKED.SYSIN DD *  
ESD ITIME  
TXT - -6& & v  
TXT -2& -2k + -Y -Y & & o <1 n o + - & -2 $  
TXT o o o ! 10 & -< o f -< o o - 0- - 0--g -qK o o & K  
TXT Y o oo . b+ o 3 -o o o 0- - 0- - 0- - q  
TXT -Y && q  
TXT / /  
TXT / /  
TXT < ERROR  
TXT 010203040506070809101112 I p s M 3 + _ 0  
END  
//GO.FT01F001 DD DUMMY  
//GO.FT02F001 DD UNIT=SYSDA,SPACE=(CYL,(15,15),RLSE),  
// DCB=(RECFM=VBS,LRECL=3516,BLKSIZE=7040,HIARCHY=1)
```

Figure 4.6 (continued)

```
//GO. FT08F001 DD DUMMY
//GO. FT09F001 DD DUMMY
//GO. FT04F001 DD UNIT=TAPE, VOL=SER=T1927, LABEL=4,
//      DSN=GITPO, DISP=OLD
//GO. SYSIN DD UNIT=SYSDA, SPACE=(TRK,(10,10)),
//      DSN='DUMY.DATA', DISP=(OLD,DELETE)
//
//
```

Figure 4.7A

Testing the Input Data for P<sub>0</sub> Case - No GIT Used

100T027GRP. COLLAPS. PO,S4 CYL.REAC. U235 FUEL

15\$ ARRAY 36 ENTRIES READ

16\* ARRAY 14 ENTRIES READ

OT

3603 LOCATIONS WILL BE USED FOR THIS PROBLEM

31143 LOCATIONS WILL BE USED TO READ CROSS SECTIONS

13\$ ARRAY 3 ENTRIES READ

OT

ELEMENTS FROM LIBRARY TAPE

1	479	URANIUM-235	ENDF
2	542	CARBON-12	ENDF
3	560	NATURAL IRON	ENDF

2\* ARRAY 27 ENTRIES READ

OT

1\* ARRAY 100 ENTRIES READ

4\* ARRAY 28 ENTRIES READ

5\* ARRAY 100 ENTRIES READ

6\* ARRAY 8 ENTRIES READ

7\* ARRAY 8 ENTRIES READ

8\$ ARRAY 27 ENTRIES READ

9\$ ARRAY 3 ENTRIES READ

10\$ ARRAY 8 ENTRIES READ

11\$ ARRAY 8 ENTRIES READ

12\* ARRAY 8 ENTRIES READ

27\$ ARRAY 5 ENTRIES READ

28\$ ARRAY 100 ENTRIES READ

OT

Figure 4.7B

Test of the Input Data for P<sub>0</sub> Case - Using GIT

100T027GRP. COLLAPS. PO,S4 CYL.REAC. U235 FUEL  
15\$ ARRAY 36 ENTRIES READ  
16\* ARRAY 14 ENTRIES READ  
OT  
3270 LOCATIONS WILL BE USED FOR THIS PROBLEM  
552 LOCATIONS WILL BE USED TO READ CROSS SECTION  
3 X-SEC. SETS READ FROM GRP. INDEPENDENT TAPE  
2\* ARRAY 27 ENTRIES READ  
OT  
1\* ARRAY 100 ENTRIES READ  
4\* ARRAY 28 ENTRIES READ  
5\* ARRAY 100 ENTRIES READ  
6\* ARRAY 8 ENTRIES READ  
7\* ARRAY 8 ENTRIES READ  
8\$ ARRAY 27 ENTRIES READ  
9\$ ARRAY 3 ENTRIES READ  
27\$ ARRAY 5 ENTRIES READ  
28\$ ARRAY 100 ENTRIES READ  
OT

A  $P_3$  treatment of the same problem may also be considered. The TAPE MAKER input cards are listed in Figure 4.8. The corresponding ANISN input data are shown in Figure 4.9. The outputs to these runs and other computer runs are available at the LSU Nuclear Science Center.

#### 4.5. DLC-37/EPR Applications

Consider a slab of the following material:

	Fe	C	Nb	Fe
Thickness (cm)	3	3	2	3
Zone	1	2	3	4
Intervals	1,2,3	4,5,6	7,8	9,10,11

Assume a source of 14.0 MeV neutrons located at the center of the third interval of C (interval number 6). It is desired to calculate the flux spectrum as well as the neutron and gamma heatings in Niobium. Neutron and gamma groups are collapsed into ten and three groups respectively. The TAPE MAKER input data is shown in Figure 4.10. As indicated, the Nb KERMA Factor is treated as a cross section data. The corresponding ANISN input data is tabulated in Figure 4.11. It should be noted that the Nb KERMA Factor is treated as an activity cross section in ANISN input data.

Figure 4.8

## TAPE MAKER Card Input for the P3 Case

```

//TMAKER3 JOB (260,7011,2,5), '44560 FARHUD'
/*SETUP T1929,T1091,T2140
//STEP1 EXEC PGM=COPIYSOUT
//SYSUT2 DD UNIT=SYSDA,SPACE=(CYL,(2,1),RLSE),
DISP=(NEW,PASS),DSN='DUMB,DAYA'
//SYSUT1 DD *
50000
100 3 4 103 32 0 12 12 0 1 2I 17
10$ 2I 13 16 4Q 4Q
20 4Q 2I 21 24 4Q
4Q
11$ 4R 0 2I 1 4 2I 9 12
4R 0 2I 9 12 4R 0 2I 1 4
2I 5 8
12* 4R 0.0 4R 1.0129-5 4R .05997 4R 0.0 4R .08479
4R 0.0 4R 7.8-6 4R .07698
13$ 479 480 481 542
543 544 545 560 561 562
563

T
// EXEC FORTGCLG,PARM.FORT='MAP',
// PARM.LKED='XREE,LIST,MAP,HIAR',
// TIME=15,REGION=(260K,200K)
//FORT.SYSPRINT DD DUMMY,SYSDA=
//FORT.SYSIN DD DSN='TAPE.MAKER',UNIT=TAPE,LABEL=11,
// VOL=SER=T2140,DISP=OLD
//LKED.SYSIN DD *
HIARCHY 1,AAA
ENTRY MAIN

```

Figure 4.8 (continued)

```
//GO.FT01F001 DD UNIT=SYSDA,SPACE=(CYL,(10,10),RLSE)),  
//   DCB=(RECFM=VBS,LRECL=80,BLKSIZE=3200  
//GO.FT02F001 DD UNIT=SYSDA,SPACE=(CYL,(10,10),RLSE)),  
//   DCB=(RECFM=VBS,LRECL=80,BLKSIZE=3200)  
//GO.FT04F001 DD UNIT=SYSDA,SPACE=(CYL,(10,10),RLSE)),  
//   DCB=(RECFM=VBS,LRECL=80,BLKSIZE=3200)  
//GO.FT08F001 DD UNIT=TAPE,VOL=(,RETAIN,SER=T1091),  
//   LABEL=8,DSN='GIT.P3',DISP=(NEW,PASS),  
//   DCB=(RECFM=VBS,LRECL=80,BLKSIZE=3200)  
//GO.FT09F001 DD UNIT=TAPE,DSN='DIC2D.UNFORM',LABEL=1,  
//   VOL=SER=T1929,DISP=OLD  
//GO.SYSIN DD UNIT=SYSDA,SPACE=(TRK,(10,10)),  
//   DSN='DUMY.DATA',DISP=(OLD,DELETE)  
//   EXEC TAPEMAP,VOL=T1091
```

Figure 4.9

ANISN P<sub>3</sub> Data for the Problem in Figure 4.1

100T027GRP.	COLLAPS.	P3,S4	CYL.REAC.	U235 FUEL				
15\$	1	0	3	27	4	2		
	0	3			1	100		
	4	103	0		0	12		
	0	0	0	0	0	0		
	0	1	0	0	0	6		
	1	3	0	0	0	1		
0								
16*	1.3	0.0	.0001	1.4209	168.			
	170.0	0.0	0.0	0.5	.001			
	.05	.001	.75					
T	9R	1.1E-6	0.017R	2.5E-5				
2*								
T								
1*	5-4.12166	4-1.13325	4-2.77033	4-6.09152	3-1.21752			
3-2.23311	3-3.79104	3-6.00338	3-8.93037	2-1.25583	2-1.67906			
2-2.14541	2-2.63197	2-3.11313	2-3.56364	2-3.96133	2-4.28906			
2-4.53567	2-4.6962	2-4.77125	2-4.76601	2-4.68902	2-4.55093			
2-4.36340	2-4.13815	2-3.88629	2-3.61787	2-3.34159	2-3.06470			
2-2.79301	2-2.53096	2-2.28182	2-2.04779	2-1.83021	2-1.62967			
2-1.44631	2-1.27972	2-1.12926	3-9.94080	3-8.73164	3-7.65445			
3-6.69823	3-5.85207	3-5.10541	3-4.44822	3-3.87106	3-3.36522			
3-2.92267	3-2.53612	3-4.95894	3-3.45783	3-2.40338	3-1.66632			
3-1.15306	4-7.96687	4-5.49814	4-3.79095	F0.0				
4*	9I	0.016I	10.0	180.0				
5*	F1.0							
6*	0.0	2R	.166667	0.0	4R	.166667		
7*	-0.471405	-0.333333	0.333333	-0.942809	-0.881917			
	0.333333	0.881917						



Figure 4.9 (continued)

8\$	9R	1	217R	3		0
9\$		1	5	9		5
19\$		3	3	3		11
27\$		2	3	4	30	17
28\$	2R	1 2R	2 2R	3 2R	4 2R	23
2R	6 2R	7 2R	8 2R	9 2R	10 2R	
2R	12 2R	13 2R	14 4R	15 4R	16 13R	
8R	18 6R	19 7R	20 7R	21 5R	22 4R	
5R	24 4R	25 4R	26	27		
T						
T						
ANISN PROB. - CYL. REACTOR NEUTRONICS P3						
15\$		1000001	0	3	4	2
	1	0	3	27	1	27
	3	4	30	0	0	0
	12	0	0	0	0	0
	30	0	0	0	0	5
	0	1	2	0	2	0
	0					
16*		1.3	0.0	.0001	1.4209	168.
		0.0	1.0	0.0	0.5	.001
		.001	.75			
T						
1*	3-.154537	3-.886180	2-.34506	2-.97944	1-.214884	
1-.38245	1-.57451	1-.75249	1-.88248	1-.94674	1-.9455	
1-.89143	1-.80244	1-.69595	.106705	1-.6954	1-.85223	
1-.153651	F0.0					
2*	9R	1.1E-6	0.017R	2.5E-5		
4*	9I	0.016I	10.0	180.0		
5*	F1.0					
6*		0.0 2R	.166667	0.0 4R	.166667	
7*		-0.471405	-0.333333	0.333333	-0.942809	-0.881917

Figure 4.9 (continued)

8\$	-0.333333	9R	0.333333	1	0.881917	217R	3
9\$				1		5	9
19\$				3		3	3
24\$			F0.0				
T							
T							



Figure 4.11

ANISN P<sub>3</sub> Data for EPR Problem

121 GROUP COLLAPSING TO 13-- PLASMA									
15\$	0	10	0	0	3	4	1	121	1
	3	0	5	11	0	0	19	19	
	19	4	124	0	0	0	6	6	
	40	0	0	0	3	1	3	3	
	2	0	1	3	0	1	1	1	
	0	0	3	0	0	1	1	1	
16*	0.0	0.0	0.0	0.0001	1.420892	50.0			
	11.0	0.0	1.0	0.0	0.5	.001			
	0.05	0.001	0.75						
T	20R1.0	F 0.0							
18*	T	F 1.0							
3*	T	F 0.0							
1*	10I0.0	11.0							
4*	F1.0	0.16666666 2R0.3333333 0.16666666							
5*	0.0	-0.881917 -0.333333 2M							
6*	-1.0								
7*	3R	1 2R	2	3 2R	4	3R	5		
8\$	5R	1	5	9	16	1			
9\$		3							
19\$		1	5	16					
22\$		3	8	18					
23\$		2	3	4					
27\$	4R	123R	222R	3 9R	16	4 9R	0		
28\$	6R	7 9R	8 4R	9	4 9R	1016R	5		
10R							11		



## CHAPTER FIVE

### Conclusions and Suggestions for Further Study

One of the major sources of error in particle transport studies is the lack of accuracy in the cross-section data. The point cross-section master library, ENDF/B, cannot be used directly in the transport computer codes, and must be averaged over a specified energy group structure. The difficulty in doing so is actually two-fold. These cross sections must be averaged to a fine-group structure using a flux spectrum that would be appropriate for a large class of neutronics systems without introducing a significant amount of inaccuracy. The next step is to flux-weight these data further for use in the particular system under investigation. The two collapsing processes must be consistent with respect to the type of flux spectra used. Furthermore, the weighting fluxes must be calculated using an accurate method that takes into account the geometry of the system, the type of the source distribution, and the degree of inhomogeneity

The temperature correction factors and resonance corrections are applied for a certain temperature when the fine-group libraries are created. If it is desired to use these cross sections in systems at different temperatures, then temperature corrections must be made to the thermal-group data.

Two fine-group libraries have been made operable at LSU as part of this thesis by converting them into unformatted cross-section tapes or ANISN Binary Tapes (ABT). These are the DLC-2D 100-group

Neutron Cross sections for use with fission spectra, and the DLC-37/EPR 100-group Neutron 21-group Gamma cross sections to be used in fusion systems and neutron and gamma heating problems.

The APRFX-I code used to collapse the DLC-2D cross sections is not capable of accurately describing the system configuration and uses the rather inaccurate diffusion theory solution to calculate the weighting fluxes. Its use is limited to the homogenous media and can only be used in conjunction with the DLC-2D data.

The ANISN code, on the other hand, is a more powerful tool in collapsing the fine-group cross sections. Any cross-section set may be collapsed using ANISN and its auxiliary code, TAPE MAKER. These collapsed cross sections may be used in any transport code which allows the ANISN-formatted input.

The modifications made to TAPE MAKER code by the author have made it possible to use higher orders of  $P_\ell$  and more energy groups in calculations. In addition, the auxiliary scanning programs developed in the preparation of this thesis have made it easier to examine the input data for TAPE MAKER and ANISN in a very short amount of CPU time. As a result of this work, it is now possible at LSU to conduct research that utilizes transport computer codes in the study of rather complicated systems composed of many regions and mixtures. A useful follow-up to the present work would be research in fission and fusion systems pertaining to neutron radiation damage, first-wall integrity in fusion systems, tritium production in lithium blankets, neutron activation calculations, and neutron and gamma

heating studies. Yet another avenue for research could now result from the development of the AMPX Modular Code System at LSU in conjunction with the ENDF/B point cross-section libraries. The eventual product would be fine-group cross-section libraries that incorporate coupled data sets for neutrons and gamma rays. Other computer codes and techniques used in resonance correcting and collapsing these data sets should be investigated for improvements and optimization in preparation of broad-group cross-section sets.



## REFERENCES

1. W. W. Engle, Jr., "A Users Manual for ANISN, A One-dimensional Discrete Ordinates Transport Code with Anisotropic Scattering," K-1693, CTC, UCC-ND (1973).
2. P. S. Pickard, "Neutron Cross-section Collapsing Code, APRFX-I," Memo for Record, AMXRD-BNL (1970).
3. N. M. Greene, et al., "AMPX: A Modular Code System for Generating Coupled Multigroup Neutron-gamma Libraries from ENDF/B," ORNL-TM-3706, ORNL (1976).
4. O. Ozer and D. Garber, "ENDF/B Summary Documentation," (for ENDF/B-III) BNL-17541 (ENDF-201) (1972).
5. M. K. Drake, Editor, "Data Formats and Procedures for the ENDF Neutron Cross-section Library," BNL-50274 (T-601) (ENDF-102, Vol. 1) (1970).
6. "100-group Neutron Cross-section Data Based on ENDF/B," (DLC-2D), RSIC Data Library Collection, ORNL (1972).
7. D. M. Plaster, R. T. Santoro, and W. E. Ford, III, "Coupled 100-group Neutron and 21-group Gamma-ray Cross-sections for EPR Calculations," ORNL-TM-5249, ORNL (1976).
8. W. W. Engle, Jr., Ref. 1, pp. 69-70 (1973).
9. R. Q. Wright, N. M. Greene, J. L. Lucius, and C. W. Craven, Jr., "SUPERTO: A Program to Generate Fine-group Constants and P<sup>n</sup> Scattering Matrices from ENDF/B," ORNL-TM-2679 (1969).
10. G. D. Joanov and J. J. Dudek, "GAM-II: A B<sub>3</sub> Code for the Calculation of Fast-neutron Spectra and Associated Multigroup Constants," GA-4265, pp. 42-46.
11. R. T. Santoro, "Neutronics Calculations for the Tokamak Experimental Power Reactor Reference Design," ORNL-TM-5033, ORNL (1975).
12. M. A. Abdu, "Computational Methods for Nuclear Heating," Ph.D Thesis, University Microfilms Inc., 74-8981.
13. W. A. Rhoads and F. R. Mynatt, "The DOT-III Two-dimensional Discrete Ordinates Transport Code," ORNL-TM-4280, ORNL (1973).

14. F. A. Straker, et al., "The MORSE Code - A Multigroup Neutron and Gamma-ray Monte Carlo Transport Code," ORNL-TM-4585, ORNL (1970).
15. J. R. Lamarsh, "Introduction to Nuclear Reactor Theory," Addison-Wesley Pub. Co. Inc., Copyright 1966.
16. G. I. Bell and S. Glasstone, "Nuclear Reactor Theory," Van Nostrand Reinhold Co., 1970.
17. G. I. Bell and S. Glasstone, Ref. 16, pages 245-247.
18. P. S. Pickard, Ref. 2, page 9.
19. J. R. Lamarsh, Ref. 15, page 54.
20. IBM System/360: "Principles of Operation," GA 22-6821.
21. LSU - SNCC, "User's Guide for the IBM System 360/65 Computer, (1976).
22. W. W. Engle, Jr., Ref. 1, page 52.
23. W. W. Engle, Jr., Ref. 1, page III.29.
24. R. M. Wyatt, "The Neutron Environment of a Cf-252 Facility," M. S. Thesis, LSU, (1972).
25. W. W. Engle, Jr., Ref. 1, page III.22.
26. J. E. Morel, "A Comparison of Calculated and Measured Cf-252 Neutron Spectra," Appen. B: "Aids and Input for ANISN," M. S. Thesis, LSU (1974).
27. E. J. Landry, "Discrete Ordinates Treatment of a Small Subcritical Assembly," Appen. B: "Supplement to User's Manual for DOT," M. S. Thesis, LSU (1972).
28. R. M. Wyatt, "The Neutron Environment of a Cf-252 Facility," Appen. A: "Supplement to MORSE User's Manual," M. S. Thesis, LSU (1972).
29. J. R. Lamarsh, Ref. 15, page 291.

APPENDIX A

Fission Sources for Several Isotopes for the 99-group  
Energy Structure of DLC-2D Library

Group	Source	Group	Source
<u>U-233 Fission Source</u>			
1	3.51793996-5	51	3.54065996-3
2	9.84442985-5	52	2.46145996-3
3	2.44521996-4	53	1.70685999-3
4	5.45474994-4	54	1.18125999-3
5	1.10456999-3	55	8.16252995-4
6	2.04995999-3	56	5.63359994-4
7	3.51742998-3	57	3.88456997-4
8	5.62406993-3	58	0.
9	8.43932986-3	59	0.
10	1.19615999-2	60	0.
11	1.61068998-2	61	0.
12	2.07130998-2	62	0.
13	2.55585998-2	63	0.
14	3.03897998-2	64	0.
15	3.49524999-2	65	0.
16	3.90193996-2	66	0.
17	4.24106991-2	67	0.
18	4.50054997-2	68	0.
19	4.67448997-2	69	0.
20	4.76267993-2	70	0.
21	4.76962996-2	71	0.
22	4.70342994-2	72	0.
23	4.57442999-2	73	0.
24	4.39418995-2	74	0.
25	4.17442995-2	75	0.
26	3.92637998-2	76	0.
27	3.66024998-2	77	0.
28	3.38495997-2	78	0.
29	3.10797998-2	79	0.
30	2.83532998-2	80	0.
31	2.57167995-2	81	0.
32	2.32045999-2	82	0.
33	2.08402997-2	83	0.
34	1.86385998-2	84	0.
35	1.66066998-2	85	0.
36	1.47461998-2	86	0.
37	1.30542000-2	87	0.
38	1.15246999-2	88	0.

Fission Sources for Several Isotopes for the 99-group  
Energy Structure of DLC-2D Library

---

Group	Source	Group	Source
<u>U-233 Fission Source (continued)</u>			
39	1.01492000-2	89	0.
40	8.91796982-3	90	0.
41	7.82039994-3	91	0.
42	6.84550995-3	92	0.
43	5.98236996-3	93	0.
44	5.22037995-3	94	0.
45	4.54939991-3	95	0.
46	3.95991996-3	96	0.
47	3.44308996-3	97	0.
48	2.99078995-3	98	0.
49	2.59561998-3	99	0.
50	5.07637995-3		

---

Fission Sources for Several Isotopes for the 99-group  
Energy Structure of DLC-2D Library

Group	Source	Group	Source
<u>U-235 Fission Source</u>			
1	4.12165993-5	51	3.88628998-2
2	1.13324998-4	52	2.40337995-3
3	2.77032998-4	53	1.66631998-3
4	6.09151995-4	54	1.15305997-3
5	1.21751998-3	55	7.96686995-4
6	2.23310998-3	56	5.49813992-4
7	3.79103997-3	57	3.79094997-4
8	6.00337994-3	58	0.
9	8.93036997-3	59	0.
10	1.25582999-2	60	0.
11	1.67905997-2	61	0.
12	2.14540997-2	62	0.
13	2.63196996-2	63	0.
14	3.11312997-2	64	0.
15	3.56363997-2	65	0.
16	3.96132994-2	66	0.
17	4.28905994-2	67	0.
18	4.53566992-2	68	0.
19	4.69619995-2	69	0.
20	4.77124995-2	70	0.
21	4.76600993-2	71	0.
22	4.68901992-2	72	0.
23	4.55092996-2	73	0.
24	4.36339992-2	74	0.
25	4.13814992-2	75	0.
26	3.88628998-2	76	0.
27	3.61786994-2	77	0.
28	3.34158996-2	78	0.
29	3.06469998-2	79	0.
30	2.79301000-2	80	0.
31	2.53095999-2	81	0.
32	2.28181997-2	82	0.
33	2.04778996-2	83	0.
34	1.83020997-2	84	0.
35	1.62968998-2	85	0.
36	1.44630998-2	86	0.
37	1.27971998-2	87	0.
38	1.12925999-2	88	0.
39	9.94079983-3	89	0.
40	8.73163986-3	90	0.

Fission Sources for Several Isotopes for the 99-group  
Energy Structure of DLC-2D Library

---

Group	Source	Group	Source
<u>U-235 Fission Source (continued)</u>			
41	7.65444994-3	91	0.
42	6.69822997-3	92	0.
43	5.85206997-3	93	0.
44	5.10540992-3	94	0.
45	4.44821995-3	95	0.
46	3.87105995-3	96	0.
47	3.36521995-3	97	0.
48	2.92266998-3	98	0.
49	2.53611997-3	99	0.
50	4.95893997-3		

---

Fission Sources for Several Isotopes for the 99-group  
Energy Structure of DLC-2D Library

Group	Source	Group	Source
<u>Pu-239 Fission Source</u>			
1	5.06228995-5	51	3.45138997-3
2	1.35049999-4	52	2.39935997-3
3	3.21494997-4	53	1.66377999-3
4	6.90658998-4	54	1.15143999-3
5	1.35262997-3	55	7.95642996-4
6	2.43729997-3	56	5.49133992-4
7	4.07442993-3	57	3.78647995-4
8	6.36674994-3	58	0.
9	9.36279988-3	59	0.
10	1.30374999-2	60	0.
11	1.72854999-2	61	0.
12	2.19297996-2	62	0.
13	2.67424998-2	63	0.
14	3.14731997-2	64	0.
15	3.58783996-2	65	0.
16	3.97464994-2	66	0.
17	4.29156995-2	67	0.
18	4.52826995-2	68	0.
19	4.68035996-2	69	0.
20	4.74875993-2	70	0.
21	4.73875999-2	71	0.
22	4.65880990-2	72	0.
23	4.51937997-2	73	0.
24	4.33182991-2	74	0.
25	4.10759997-2	75	0.
26	3.85750997-2	76	0.
27	3.59134993-2	77	0.
28	3.31758994-2	78	0.
29	3.04330999-2	79	0.
30	2.77418998-2	80	0.
31	2.51460999-2	81	0.
32	2.26773998-2	82	0.
33	2.03576997-2	83	0.
34	1.82001998-2	84	0.
35	1.62110999-2	85	0.
36	1.43911998-2	86	0.
37	1.27372998-2	87	0.
38	1.12428999-2	88	0.
39	9.89958990-3	89	0.
40	8.69761980-3	90	0.

Fission Sources for Several Isotopes for the 99-group  
Energy Structure of DLC-2D Library

Group	Source	Group	Source
<u>Pu-239 Fission Source (continued)</u>			
41	7.62640995-3	91	0.
42	6.67514992-3	92	0.
43	5.83310992-3	93	0.
44	5.08984995-3	94	0.
45	4.43543988-3	95	0.
46	3.86057997-3	96	0.
47	3.35660997-3	97	0.
48	2.91559997-3	98	0.
49	2.53030998-3	99	0.
50	4.94851995-3		



Fission Sources for Several Isotopes for the 99-group  
Energy Structure of DLC-2D Library

Group	Source	Group	Source
<u>Pu-241 Fission Source</u>			
1	5.94814992-5	51	3.29129997-3
2	1.56710999-4	52	2.28679997-3
3	3.68644997-4	53	1.58502999-3
4	7.83022994-4	54	1.09656999-3
5	1.51705998-3	55	7.57524997-4
6	2.70567995-3	56	5.22716993-4
7	4.47914994-3	57	3.60373995-4
8	6.93450993-3	58	0.
9	1.01081999-2	59	0.
10	1.39581999-2	60	0.
11	1.83597998-2	61	0.
12	2.31180999-2	62	0.
13	2.79914999-2	63	0.
14	3.27218997-2	64	0.
15	3.70650998-2	65	0.
16	4.08152997-2	66	0.
17	4.38211995-2	67	0.
18	4.59928995-2	68	0.
19	4.73007995-2	69	0.
20	4.77678996-2	70	0.
21	4.74587995-2	71	0.
22	4.64675999-2	72	0.
23	4.49050993-2	73	0.
24	4.28889996-2	74	0.
25	4.05347997-2	75	0.
26	3.79503995-2	76	0.
27	3.52316996-2	77	0.
28	3.24607998-2	78	0.
29	2.97050998-2	79	0.
30	2.70178998-2	80	0.
31	2.44393995-2	81	0.
32	2.19984999-2	82	0.
33	1.97139999-2	83	0.
34	1.75965998-2	84	0.
35	1.56505999-2	85	0.
36	1.38750999-2	86	0.
37	1.22653998-2	87	0.
38	1.08142999-2	88	0.
39	9.51253986-3	89	0.
40	8.34978986-3	90	0.

Fission Sources for Several Isotopes for the 99-group  
Energy Structure of DLC-2D Library

---

Group	Source	Group	Source
<u>Pu-241 Fission Source (continued)</u>			
41	7.31521994-3	91	0.
42	6.39783996-3	92	0.
43	5.58684999-3	93	0.
44	4.87183994-3	94	0.
45	4.24299991-3	95	0.
46	3.69111997-3	96	0.
47	3.20772997-3	97	0.
48	2.78506997-3	98	0.
49	2.41606998-3	99	0.
50	4.72235996-3		

---

Fission Sources for Several Isotopes for the 99-group  
Energy Structure of DLC-2D Library

Group	Source	Group	Source
<u>Cf-252 Fission Source</u>			
1	2.11560997-4	51	2.68588996-3
2	4.81211996-4	52	1.86336999-3
3	9.91409993-4	53	1.29004999-3
4	1.86835998-3	54	8.91687989-4
5	3.24963999-3	55	6.15560991-4
6	5.25856996-3	56	4.24525994-4
7	7.97483987-3	57	2.92553997-4
8	1.14091998-2	58	0.
9	1.54893999-2	59	0.
10	2.00627998-2	60	0.
11	2.49124998-2	61	0.
12	2.97849998-2	62	0.
13	3.44215998-2	63	0.
14	3.85871997-2	64	0.
15	4.20929998-2	65	0.
16	4.48085994-2	66	0.
17	4.66665995-2	67	0.
18	4.76579994-2	68	0.
19	4.78235990-2	69	0.
20	4.72410995-2	70	0.
21	4.60134995-2	71	0.
22	4.42563993-2	72	0.
23	4.20884997-2	73	0.
24	3.96239999-2	74	0.
25	3.69672999-2	75	0.
26	3.42097998-2	76	0.
27	3.14282998-2	77	0.
28	2.86850998-2	78	0.
29	2.60282999-2	79	0.
30	2.34938997-2	80	0.
31	2.11062998-2	81	0.
32	1.88811998-2	82	0.
33	1.68263997-2	83	0.
34	1.49438998-2	84	0.
35	1.32312998-2	85	0.
36	1.16824998-2	86	0.
37	1.02892998-2	87	0.
38	9.04196990-3	88	0.
39	7.92976987-3	89	0.
40	6.94171995-3	90	0.

Fission Sources for Several Isotopes for the 99-group  
Energy Structure of DLC-2D Library

---

Group	Source	Group	Source
<u>Cf-252 Fission Source (continued)</u>			
41	6.06680995-3	91	0.
42	5.29432994-3	92	0.
43	4.61403996-3	93	0.
44	4.01632988-3	94	0.
45	3.49224997-3	95	0.
46	3.03357998-3	96	0.
47	2.63281998-3	97	0.
48	2.28316996-3	98	0.
49	1.97853997-3	99	0.
50	3.86108997-3		

---

APPENDIX B

APRFX-I Partial Output

COLLAPSES MULTIGROUP CONSTANTS FROM ENDF/B DLC-2D  
99 GROUP LIBRARY TO A SPECIFIED INPUT STRUCTURE

NUMBER OF FINE ENERGY GROUPS . . . . .	100
LENGTH OF CROSS SECTION TABLE. . . . .	103
POSITION OF ABSORPTION CROSS SECTION . . . . .	1
NUMBER OF BROAD ENERGY GROUPS. . . . .	27
TOTAL NUMBER OF ISOTOPES TO BE READ. . . . .	5 CARDS 0 TAPE 5
INPUT(0) OR CALCULATED (GT 0) SPECTRUM . . . . .	2
BUCKLING FACTOR FOR INFINITE MEDIA CALC. . . . .	0.52800E-03
OUTPUT OPTIONS 0/1/2 NONE/PRINT/TAPE N6. . . . .	0
NUMBER OF MIXTURE CROSS SECTION SETS . . . . .	3

## APPENDIX C

### Modifications to TAPE MAKER

Aside from addition of the subroutine IMAGE to TAPE MAKER, the storage arrays in the code were broken into two parts to allow use of Low Speed Core as well as High Speed Core. This was done through changing the BLANK COMMON to a NAMED COMMON, AAA, and dimensioning DUMY (50000):

```
COMMON/AAA/D(1),LIM1,.....,DUMY(50000)
```

Then HIARCHY specification was used:

```
//LKED.SYSIN DD *  
  HIARCHY 1, AAA  
  ENTRY MAIN
```

where HIARCHY 1 implies Low Core allocation. The //LKED.SYSIN DD \* card follows the //FORT.SYSIN DD card immediately.

## APPENDIX D

### Creating a LOAD MODULE of ANISN

```
//LOADMOD JOB (150,7011,10,5),'44560 FARHUD'  
/*SETUP T1522  
// EXEC FORTGCL,TIME.FORT=10,PARM.FORT='NO SOURCE',PARM.LKED='XREF,  
// LET,LIST,OVL,SIZE=(150000,12000)',REGION.LKED=150K  
//FORT.SYSIN DD UNIT=TAPE,VOL=SER=T1522,LABEL=17,DSN=ANISN,DISP=OLD  
//LKED.SYSLMOD DD VOL=SER=LSU005,DSN=NSMILE.LOADS,DISP=(NEW,CATLG),  
// SPACE=(TRK,(25,5,5))  
//LKED.SYSIN DD *  
ENTRY MAIN  
OVERLAY LEVEL 1  
INSERT PLSNT,FIDO,TP,ADJNT,S804,S805,S814,WOT8,S966,FFREAD  
OVERLAY LEVEL 1  
INSERT GUTS,S807,S810,S821,S824,S833,DT,CELL,S851  
OVERLAY LEVEL 1  
INSERT FINPR,FINPR1,PUNSH,DTFPUN,FLTFX  
OVERLAY LEVEL 2  
INSERT BT,SUMMARY,FACTOR  
OVERLAY LEVEL 2  
INSERT FEWG,WATE  
OVERLAY LEVEL 3 (REGION)  
NAME ANISN(R)  
//
```

FORTTRAN Compile and Link options are invoked in EXEC statement. The ANISN program is accessed via //FORT.SYSIN DD card. The final LOAD MODULE is created by //LKED.SYSLMOD DD statement and is placed on the Disk Pack LSU005 with DSN=NSMILE.LOADS. The OVERLAY Structure follows the //LKED.SYSIN DD \* card.

## VITA

Farhad Dolatshahi was born in Tehran, Iran on October 23, 1950. He received his high school diploma in mathematics and science in 1969. In 1975 he received the degree of Bachelor of Science in Physics from Illinois Institute of Technology. In August 1975 he transferred to Louisiana State University where he is presently a candidate for the degree of Master of Science in the Department of Nuclear Engineering.

He is a student member of the American Nuclear Society and also Sigma Pi Sigma.



EXAMINATION AND THESIS REPORT

Candidate: Farhad Dolatshahi

Major Field: Nuclear Engineering

Title of Thesis: Preparation of Broad-group Cross Sections for Multigroup  
Transport Calculations - ANISN Computer Code Options

Approved:

*Robert E. Miles*

Major Professor and Chairman

Dean of the Graduate School

EXAMINING COMMITTEE:

*John C. Courtney*

*Robert C. McHenry*

*Frank A. Selding*

Date of Examination:

December 29, 1977